Table of Content of Supplementary Data

Fig.S1 Small RNA sequencing of renal IM, validation parameters

A

	Read count mean		Percentage of previous category	
	Ctr	Dicer^{AQP2CRE}	Ctr	Dicer^{AQP2CRE}
Total	**(13786877 - 15471919)**			
Adapter Trimmed	**(13113937 - 14448741)**		**(95,1% - 93,4%)**	
Length and quality filtered	**(11329358 - 12326885)**		**(86,4% - 85,3%)**	
Mapped reads to genome (mm9)	**(7987420 - 8011973)**		**(70,5% - 64,9%)**	
Mapped to miRBase (v.21)	**(5946030 - 5397065)**		**(74,4% - 67,4%)**	

B

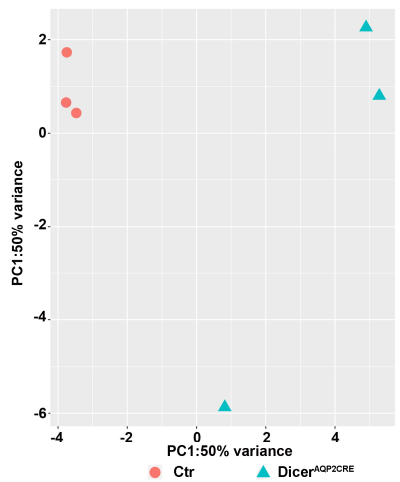

Panel A shows a summary table of the identified reads. 1 µg of RNA from inner medulla (IM; n: 3 vs 3) was processed according to a TruSeq small-RNA (ILLUMINA) protocol in order to obtain 50 base pair single-reads on the Illumina HiSeq2500 Platform. Using iMir software, the reads were trimmed, mapped to the mice genome (mm9), and annotated. In panel B, a two dimensional PCA analysis of samples from control (red circles) and DicerAQP2-CRE mice (blue triangles) show complete group segregation

Fig.S2 Predicted transcription and epigenetic factors targeted by miR7688-5p, miR-409-3p and miR-8114.

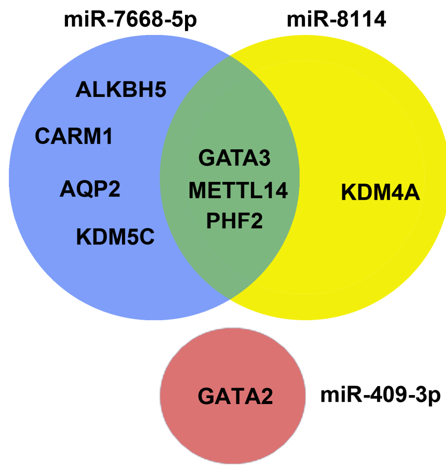

Blue Circle includes the putative targets of miR-7688-5p, while yellow circle the ones of miR-8114. Some of the targets were in common (green interception). Target of miR-409-3p is shown in a red circle.

Fig.S3 Transfection efficiency

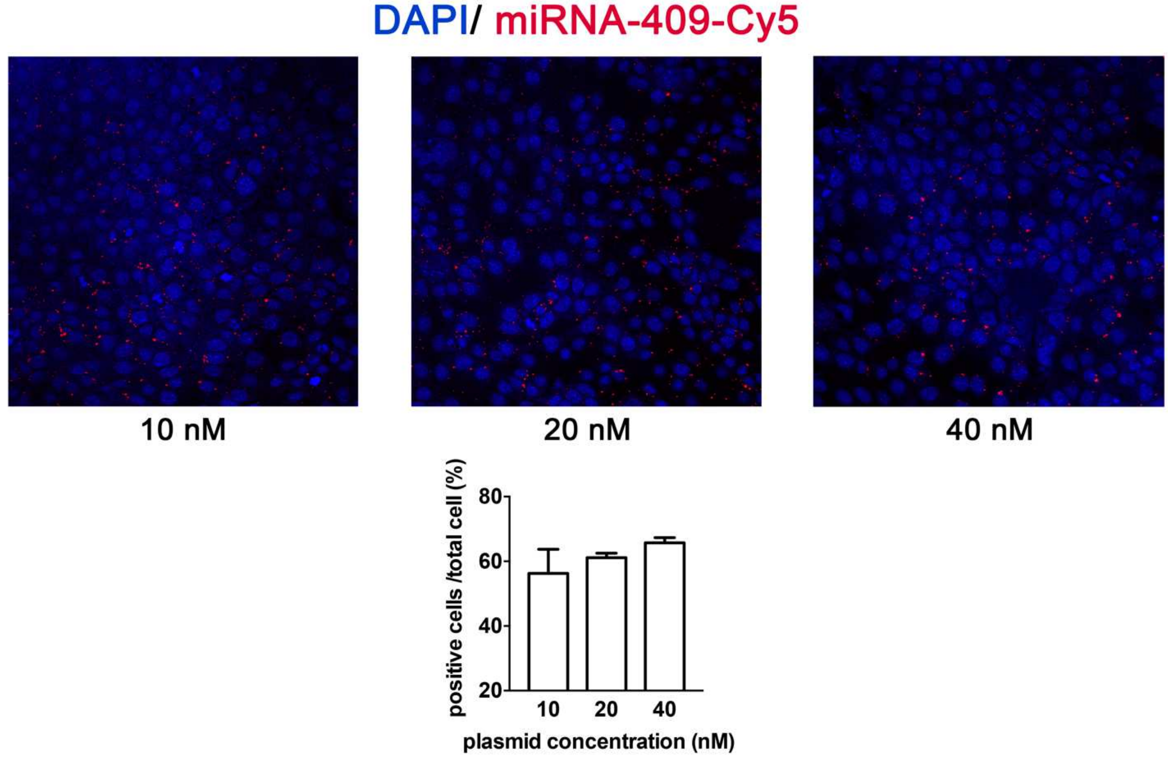

Transfection efficiency was evaluated by testing different concentrations of lipofectamine (1:1 and 1:2) along with three different concentrations (10, 20, and 40 nM) of a testing Cy5-conjugated miRNA-409. In the graph, it is reported the percentage of cells positive to the Cy5-conjugated miRNA-409 signal over the total number of nucleated cells. Lipofectamine concentration 1:2 was considered optimal and the figure refers to this condition.

Fig.S4 Renal Fibrosis evaluation

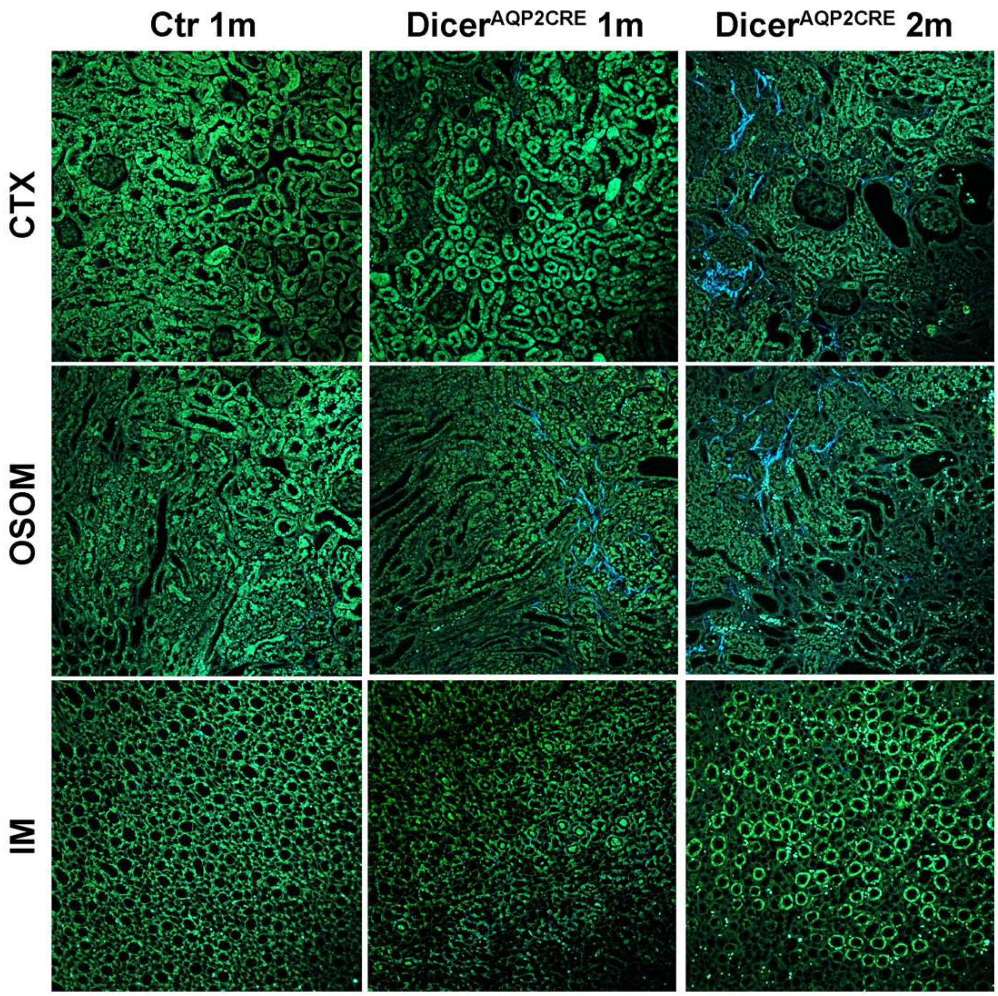

Representative pictures from cortex (CTX), outer stripe of outer medulla (OSOM) and inner medulla (IM) of renal parenchyma (green) and fibrillar collagen (blue) acquired at label-free 2 photon microscope by generating second armonic signal. Fibrillar collagen was detectable mainly in 2 months old DicerAQP2CRE mice (CTX and OSOM; picture magnification 20X).

Fig.S5 Localization of phosphorylated (pSer256) AQP2 in inner medulla

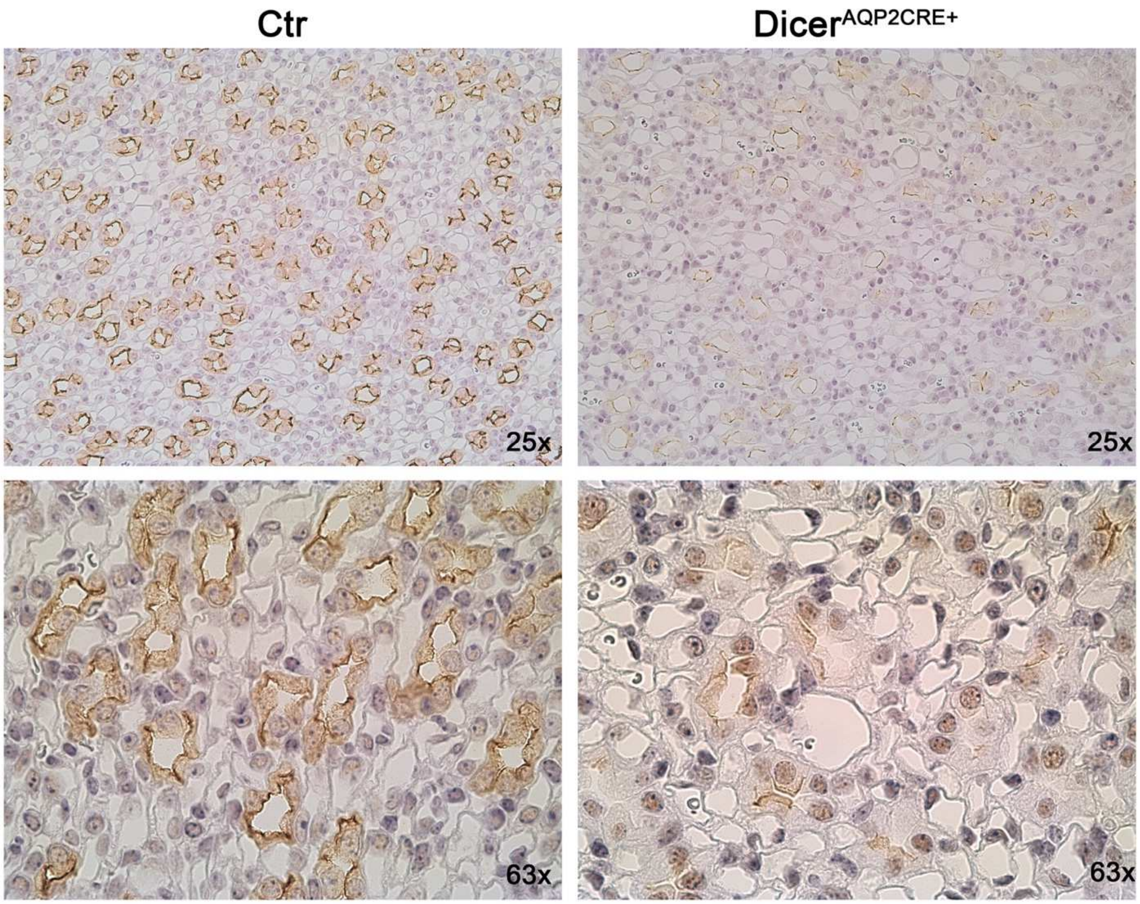

Representative pictures of renal inner medulla from Ctr and DicerAQP2Cre+ mice stained with an anti-pS256 AQP2 antibody. Upper panel represent low magnification and lower panels high magnification pictures. The signal is severely downregulated in DicerAQP2Cre+ mice, however, residual expression in some scattered PC reveal a proper apical localization of pS256-AQP2 signal.

Fig.S6 Immunoblotting of phosho-forms of AQP2 in mouse kidney

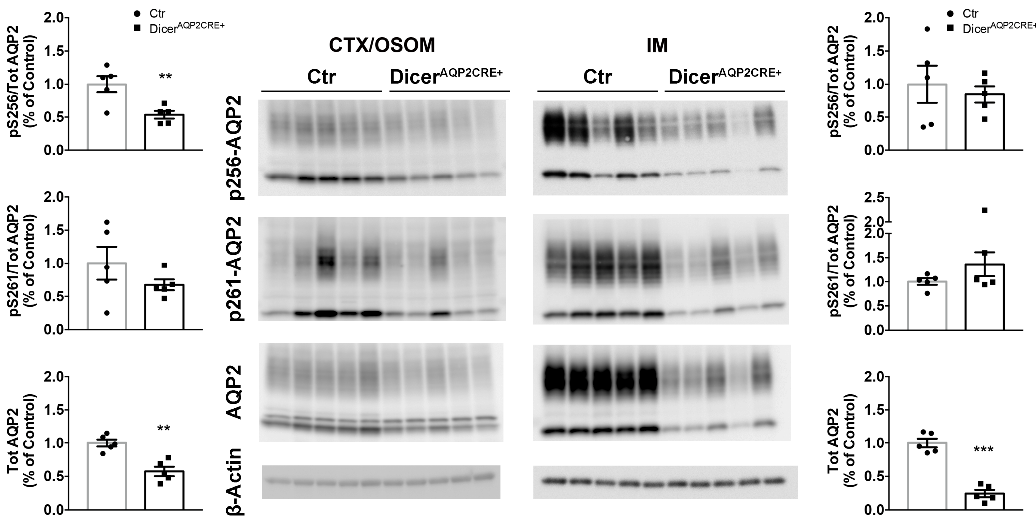

Immunoblotting from CTX/OSOM (left) and IM (right) samples of kidney from Ctr and Dicer$^{AQP2Cre+}$ mice probed for pSer256- or pSer261- AQP2 and total AQP2 antibody. The graph represents the abundance of the indicated protein as percentage of Ctr samples. The p-forms were normalized for total AQP2 abundance. Beta actin abundance was used as loading control. ** stands for p-value < 0.01. Unpaired t-test has been used for group comparison (n= 5 vs 5).

Fig.S7 Ingenuity Pathways Analysis interaction network of predicted miRNAs targets

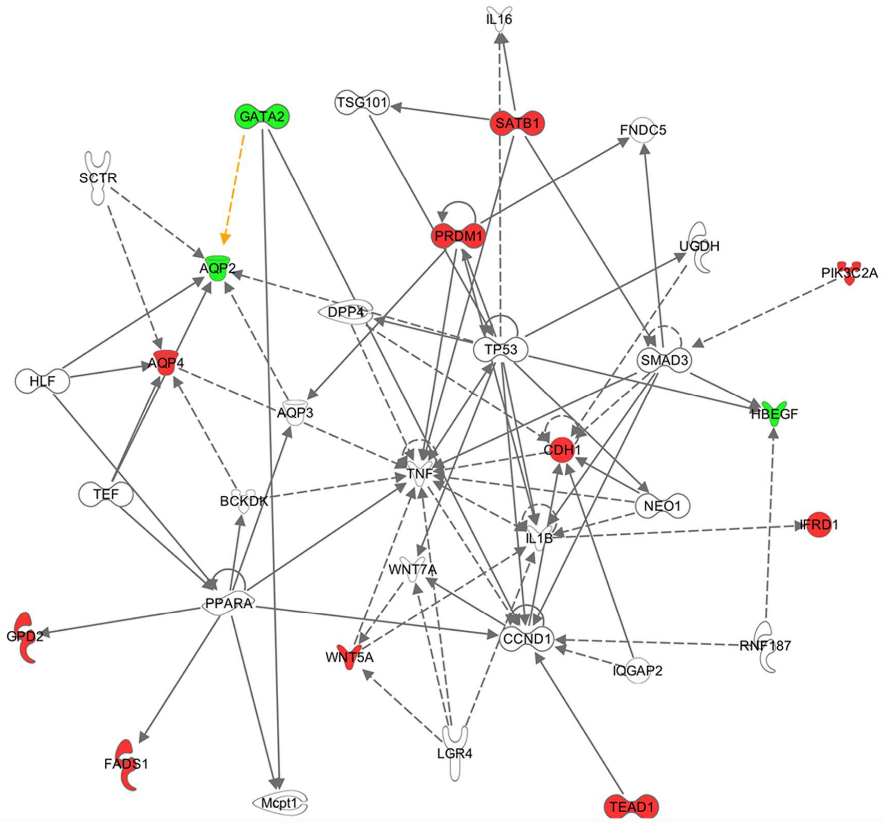

The interaction network was built by Ingenuity Pathways Analysis (IPA, www.ingenuity.com), by using as entries experimentally-validated target genes of the regulated miRNAs and filtering them for the ones over-expressed in IMCD compared to non-IMCD (http://esbl.nhlbi.nih.gov/IMCD-transcriptome/), as specific of CD. This network was centered on the external entry AQP2.

Fig.S8 Volcano plot of proteomic analysis output data

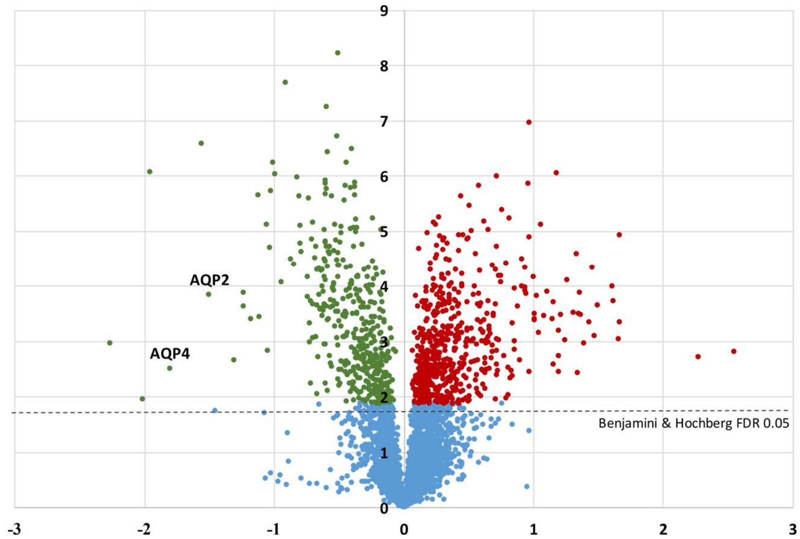

The Volcano plot was built by plotting on Y-axis: log10 (p value), X-axis: log2 (fold-change). The horizontal dashed line represents the Benjamini-Hochberg FDR threshold of 0.05. Proteins significantly decreased are indicated in green, those significantly increased in abundance are indicated in red.

Fig-S9 Immunoblotting of phosho-forms of AQP2 in mpkCCD14(c11) cells transfected with miRNAs mimics

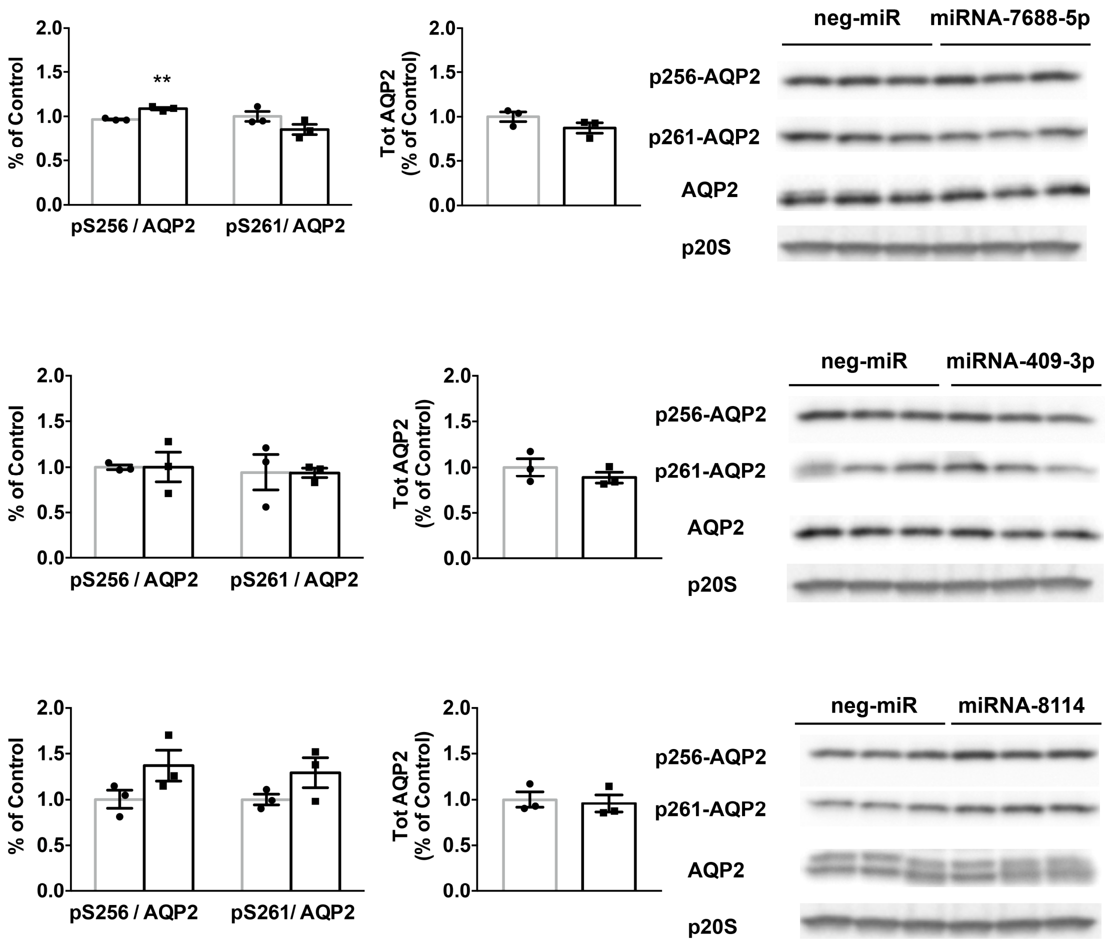

Immunoblotting from mpkCCD14(c11) cells transfected with miRNAs mimics of miR7688-5p, mir409-3p, miR8114 or neg-miR and treated for 24h with dDAVP and probed with an anti-pS256- or pS261 AQP2 antibody or anti-total AQP2 antibody. The graph indicates the protein abundance as percentage of the control (neg-miR transfection). The phosphorylated forms are normalized for the total AQP2 abundance. Expression level of p20S was used as loading control. ** is for $p < 0.01$. Unpaired t-test was used for comparison of the two groups (n= 3 vs 3).

Fig-S10 Predicted interaction sites between miR-7688-5p, miR-409-3p, miR-8114 and their putative 3’UTR regions used in the luciferase assay

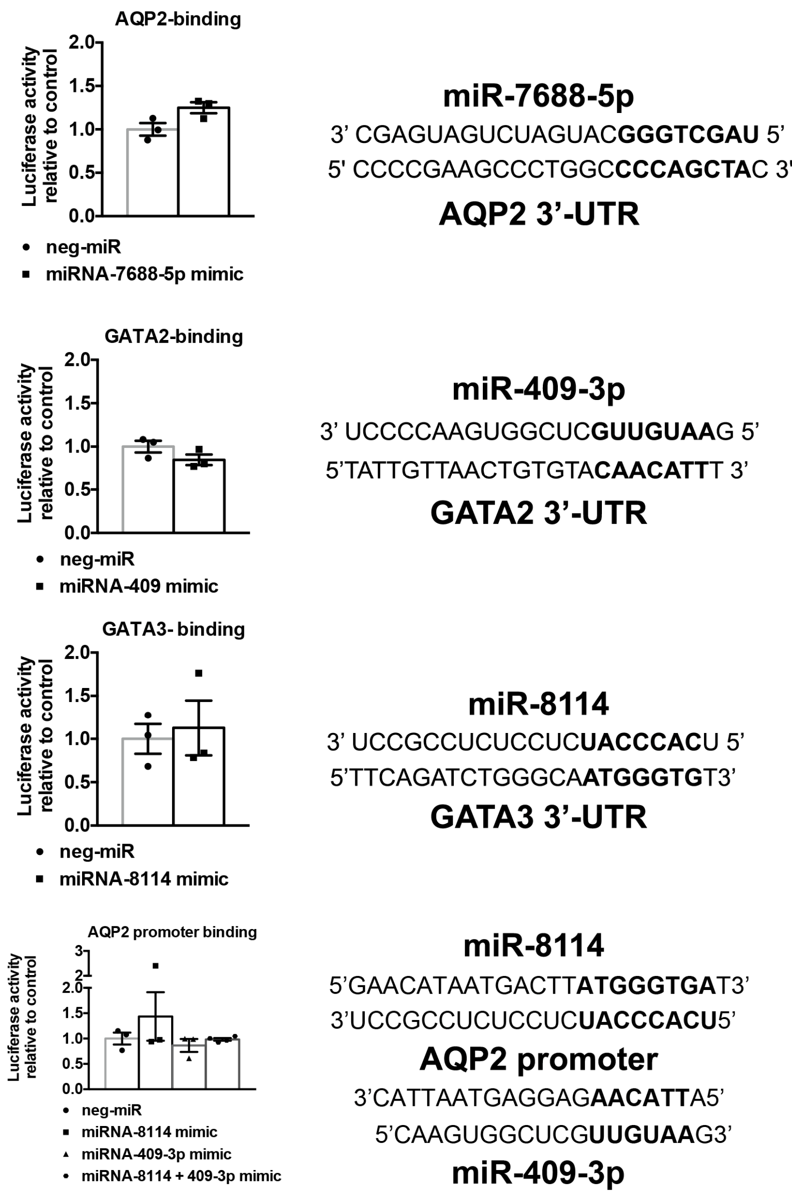

Predicted interaction sites between miR-7688-5p, mir409-3p, miR8114 and their putative 3’UTR regions used in the luciferase assay. Luciferase assay was performed in HEK cells. On the left, the bar graph reports the luciferase activity as in Fig-5. This result is matched on the right with the interaction site between the specific miRNA used and its target site at 3’UTR of the respective target mRNA. miR8114 are predicted to target also a region at the AQP2 promoter as showed in the lowest panel.

Fig.S11 Immunoblotting of Kdm5c and Phf2 expression in inner medulla

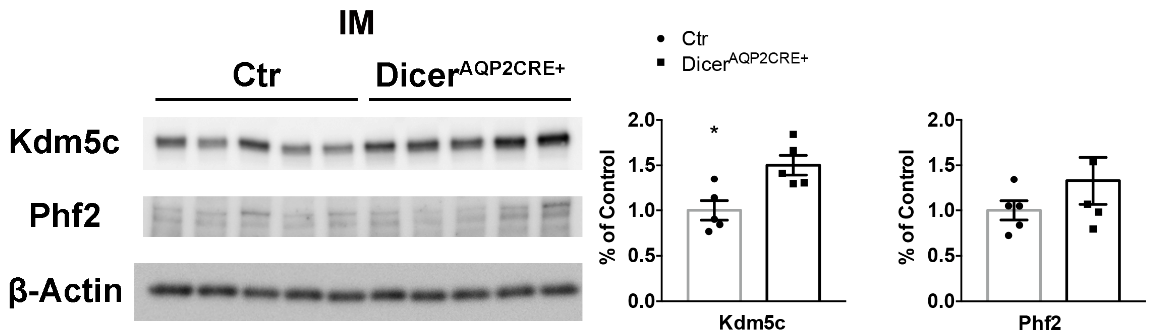

Immunoblotting of IM samples from Ctr and Dicer$^{AQP2Cre+}$ mice probed with an anti-Kdm5c and Phf2 antibody. The graph shows protein abundance as percentage of the Ctr. * is for $p < 0.05$. Unpaired t-test was used for comparison of the two groups (n= 5 vs 5).

Table-S1 List of primers

Gene	Primers sequence
Genotype	
AQP2 P1 Fw	AAGTGCCCACAGTCTAGCCTCT
AQP2 P2 Fw	CCTGTTGTTCAGCTTGCACCAG
AQP2 P3 rev	GGAGAACGCTATGGACCGGAGT
Dicer1 Fw 1	ATTGTTACCAGCGCTTAGAATTCC
Dicer1 Fw 2	TCGGAATAGGAACTTCGTTTAAAC
Dicer1 rev	GTACGTCTACAATTGTCTATG
RT-PCR	
AQP2 Fw	GCAGTTGTCACTGGCAAGTTT
AQP2 rev	AGGGGAACAGCAGGTAGTTG
Dicer Fw	ACTCAGAGAAGTGGGAAAAGGA
Dicer rev	ATTGTTACCAGCGCTTAGAATTCC
AVPR2 Fw	GACTAAGTTGGCCTCCTGTGA
AVPR2 rev	GGTCTCGGTCATCCAGTAGC
Gata2 Fw	ACCTGTGCAATGCCTGTGGG
Gata2 rev	TTGCACAACAGGTGCCCGCT
Elf3 Fw	TGGAGGGCAAGAAGAGCAAG
Elf3 rev	GCTCGGGGTGGATTAGGATG
Gata3 Fw	CTCCTCTACGCTCCTTGCTAC
Gata3 rev	GGAGAGAGGAATCCGAGTGTG
18S Fw	GGATCCATTGGAGGGCAAGT
18S rev	ACGAGCTTTTTAACTGCAGCAA
mGAPDH Fw	CTGTGGATGGCCCCTCTGGA
mGAPDH rev	GGGCCCTCAGATGCCTGCTT
β-actin Fw	GTCGAGTCGCGTCCACC
β-actin rev	GTCATCCATGGCGAACTGGT
Kdm5c Fw	TGTGCGTGCACACATAAAATAGA
Kdm5c rev	CTGGTAGGGGAGGAAGACTCA
Kdm4a Fw	AGAAAGACAGTGGGATCGGC
Kdm4a rev	AAACCTGGAGCCTAAAGCCC
Phf2 Fw	TCTCAACGTGACCAACCTCG
Phf2 rev	TCGGGCCAGTAGTTTTCCAC
mmu-mir-409-3p	CGAATGTTGCTCGGTGAAC
mmu-mir-7688-5p	GCTAGCTGGGCATGATCTGA
mmu-mir-8114	TCACCCATCTCCTCTCCG
USLP	GAAAGAAGGCGAGGAGCAGATCGAGGAAGA AGACGGAAGAATGTGCGTCTCGCCTTCTTTC NNNNNNNN

Table-S2 List of validated targets of the significantly regulated miRNAs

ID	Exp Fold Change	Source	Symbol	Target Predicted Regulation
mmu-miR-212-3p	2,57	Ingenuity Expert Findings, TarBase, TargetScan Human, miRecords	ARHGAP32	-1
mmu-miR-212-3p	2,57	miRecords	CAPN8	-1
mmu-miR-212-3p	2,57	Ingenuity Expert Findings, TargetScan Human	HBEGF	-1
mmu-miR-212-3p	2,57	TargetScan Human, miRecords	MECP2	-1
mmu-miR-212-3p	2,57	miRecords	MMP9	-1
mmu-miR-212-3p	2,57	TarBase	PGC	-1
mmu-miR-212-3p	2,57	Ingenuity Expert Findings, TargetScan Human	RB1	-1
mmu-miR-212-3p	2,57	miRecords	TJP1	-1
mmu-miR-212-3p	2,57	Ingenuity Expert Findings, TargetScan Human	TLN2	-1
mmu-miR-141-3p	-2,22	TargetScan Human, miRecords	BAP1	1
mmu-miR-141-3p	-2,22	TarBase, TargetScan Human, miRecords	CLOCK	1
mmu-miR-141-3p	-2,22	Ingenuity Expert Findings, TargetScan Human	CTBP2	1
mmu-miR-141-3p	-2,22	miRecords	CTNNB1	1
mmu-miR-141-3p	-2,22	Ingenuity Expert Findings	CYP1B1	1
mmu-miR-141-3p	-2,22	miRecords	DLX5	1
mmu-miR-141-3p	-2,22	miRecords	ELMO2	1
mmu-miR-141-3p	-2,22	miRecords	ERBB2IP	1
mmu-miR-141-3p	-2,22	TarBase	GEMIN2	1
mmu-miR-141-3p	-2,22	miRecords	KLHL20	1
mmu-miR-141-3p	-2,22	TargetScan Human, miRecords	MAP2K4	1
mmu-miR-141-3p	-2,22	Ingenuity Expert Findings, TargetScan Human	PITX2	1
mmu-miR-141-3p	-2,22	TargetScan Human, miRecords	PTPRD	1
mmu-miR-141-3p	-2,22	Ingenuity Expert Findings, TargetScan Human	STAT5B	1
mmu-miR-141-3p	-2,22	TargetScan Human, miRecords	TGFB2	1
mmu-miR-141-3p	-2,22	miRecords	WDR37	1
mmu-miR-141-3p	-2,22	Ingenuity Expert Findings, TargetScan Human	YAP1	1
mmu-miR-141-3p	-2,22	TarBase, TargetScan Human, miRecords	ZEB1	1
mmu-miR-141-3p	-2,22	TarBase, TargetScan Human, miRecords	ZEB2	1
mmu-miR-141-3p	-2,22	TargetScan Human, miRecords	ZFPM2	1
mmu-miR-155-5p	-2,07	miRecords	ABHD16A	1
mmu-miR-155-5p	-2,07	Ingenuity Expert Findings, TarBase,miRecords	AGTR1	1
mmu-miR-155-5p	-2,07	TarBase, TargetScan Human, miRecords	AICDA	1
mmu-miR-155-5p	-2,07	TarBase	AMIGO2	1
mmu-miR-155-5p	-2,07	TarBase, TargetScan Human	ANKFY1	1
mmu-miR-155-5p	-2,07	TarBase	ARFIP1	1
mmu-miR-155-5p	-2,07	TarBase	ARFIP2	1
mmu-miR-155-5p	-2,07	TarBase, TargetScan Human	ARID2	1
mmu-miR-155-5p	-2,07	TarBase	ARL10	1
mmu-miR-155-5p	-2,07	TarBase, TargetScan Human	ARL5B	1
mmu-miR-155-5p	-2,07	TarBase	ATG3	1
mmu-miR-155-5p	-2,07	TarBase, TargetScan Human	ATP6V1C1	1
mmu-miR-155-5p	-2,07	Ingenuity Expert Findings, TarBase, TargetScan Human, miRecords	BACH1	1

mmu-miR-155-5p	-2,07	TarBase, TargetScan Human	BET1	1
mmu-miR-155-5p	-2,07	TarBase	BRPF3	1
mmu-miR-155-5p	-2,07	TarBase	CBFB	1
mmu-miR-155-5p	-2,07	TargetScan Human,miRecords	CCND1	1
mmu-miR-155-5p	-2,07	Ingenuity Expert Findings	CD47	1
mmu-miR-155-5p	-2,07	TarBase	CDK5RAP3	1
mmu-miR-155-5p	-2,07	Ingenuity Expert Findings, TarBase, TargetScan Human, miRecords	CEBPB	1
mmu-miR-155-5p	-2,07	TarBase, TargetScan Human	CHAF1A	1
mmu-miR-155-5p	-2,07	TarBase, TargetScan Human	CLDN1	1
mmu-miR-155-5p	-2,07	Ingenuity Expert Findings, TargetScan Human	CSF1R	1
mmu-miR-155-5p	-2,07	Ingenuity Expert Findings, TargetScan Human	CTLA4	1
mmu-miR-155-5p	-2,07	TarBase	CTNNB1	1
mmu-miR-155-5p	-2,07	TarBase	CUL4B	1
mmu-miR-155-5p	-2,07	Ingenuity Expert Findings, TargetScan Human	CUX1	1
mmu-miR-155-5p	-2,07	TarBase	CYP51A1	1
mmu-miR-155-5p	-2,07	miRecords	CYR61	1
mmu-miR-155-5p	-2,07	TarBase	DCAF7	1
mmu-miR-155-5p	-2,07	TarBase, TargetScan Human	DHX40	1
mmu-miR-155-5p	-2,07	TarBase, TargetScan Human	DNAJB1	1
mmu-miR-155-5p	-2,07	TarBase	DNAJC19	1
mmu-miR-155-5p	-2,07	TarBase	DPP7	1
mmu-miR-155-5p	-2,07	TarBase	DSG2	1
mmu-miR-155-5p	-2,07	TargetScan Human, miRecords	ETS1	1
mmu-miR-155-5p	-2,07	TarBase	F2	1
mmu-miR-155-5p	-2,07	miRecords	FADD	1
mmu-miR-155-5p	-2,07	TarBase	FADS1	1
mmu-miR-155-5p	-2,07	TarBase, TargetScan Human	FAR1	1
mmu-miR-155-5p	-2,07	Ingenuity Expert Findings, TargetScan Human, miRecords	FGF7	1
mmu-miR-155-5p	-2,07	TarBase, TargetScan Human	FMNL2	1
mmu-miR-155-5p	-2,07	TargetScan Human, miRecords	FOXO3	1
mmu-miR-155-5p	-2,07	TarBase	GNA13	1
mmu-miR-155-5p	-2,07	TarBase	HSD17B12	1
mmu-miR-155-5p	-2,07	TarBase, TargetScan Human	HSDL1	1
mmu-miR-155-5p	-2,07	TargetScan Human, miRecords	IKBKE	1
mmu-miR-155-5p	-2,07	Ingenuity Expert Findings	IL13RA1	1
mmu-miR-155-5p	-2,07	Ingenuity Expert Findings, TargetScan Human, miRecords	INPP5D	1
mmu-miR-155-5p	-2,07	Ingenuity Expert Findings, TargetScan Human, miRecords	JARID2	1
mmu-miR-155-5p	-2,07	TarBase	LCLAT1	1
mmu-miR-155-5p	-2,07	TarBase, miRecords	LDOC1	1
mmu-miR-155-5p	-2,07	TarBase	LPL	1
mmu-miR-155-5p	-2,07	TarBase	LY6K	1
mmu-miR-155-5p	-2,07	miRecords	MAF	1
mmu-miR-155-5p	-2,07	TarBase	MARC1	1
mmu-miR-155-5p	-2,07	TarBase, miRecords	MATR3	1
mmu-miR-155-5p	-2,07	TargetScan Human, miRecords	MEIS1	1
mmu-miR-155-5p	-2,07	TarBase	MET	1

mmu-miR-155-5p	-2,07	TarBase	METTL7A	1
mmu-miR-155-5p	-2,07	TarBase	MOSPD2	1
mmu-miR-155-5p	-2,07	TarBase	MPZL1	1
mmu-miR-155-5p	-2,07	TarBase	MSI2	1
mmu-miR-155-5p	-2,07	TargetScan Human, miRecords	MYB	1
mmu-miR-155-5p	-2,07	Ingenuity Expert Findings, miRecords	MYD88	1
mmu-miR-155-5p	-2,07	Ingenuity Expert Findings, TarBase, TargetScan Human	MYO10	1
mmu-miR-155-5p	-2,07	TarBase	MYO1E	1
mmu-miR-155-5p	-2,07	TarBase, TargetScan Human	NARS	1
mmu-miR-155-5p	-2,07	TarBase	NT5E	1
mmu-miR-155-5p	-2,07	TarBase	PDE3A	1
mmu-miR-155-5p	-2,07	TarBase	PDLIM5	1
mmu-miR-155-5p	-2,07	TarBase, TargetScan Human	PHC2	1
mmu-miR-155-5p	-2,07	Ingenuity Expert Findings, TarBase	PICALM	1
mmu-miR-155-5p	-2,07	TarBase, TargetScan Human	PKN2	1
mmu-miR-155-5p	-2,07	TarBase	PLXND1	1
mmu-miR-155-5p	-2,07	Ingenuity Expert Findings	PMAIP1	1
mmu-miR-155-5p	-2,07	TarBase	PODXL	1
mmu-miR-155-5p	-2,07	TarBase	POLE3	1
mmu-miR-155-5p	-2,07	TarBase	POLE4	1
mmu-miR-155-5p	-2,07	TarBase	PPL	1
mmu-miR-155-5p	-2,07	TarBase	PPP5C	1
mmu-miR-155-5p	-2,07	TarBase	PRAF2	1
mmu-miR-155-5p	-2,07	TarBase	PRKCI	1
mmu-miR-155-5p	-2,07	TarBase, TargetScan Human	PTPRJ	1
mmu-miR-155-5p	-2,07	TarBase	RAB23	1
mmu-miR-155-5p	-2,07	TarBase	RAB27B	1
mmu-miR-155-5p	-2,07	TarBase, TargetScan Human	RAB34	1
mmu-miR-155-5p	-2,07	TarBase, TargetScan Human	RAB5C	1
mmu-miR-155-5p	-2,07	TarBase, TargetScan Human	RAB6A	1
mmu-miR-155-5p	-2,07	TarBase	RAI14	1
mmu-miR-155-5p	-2,07	TarBase, TargetScan Human	RCN2	1
mmu-miR-155-5p	-2,07	TarBase, TargetScan Human	RCOR1	1
mmu-miR-155-5p	-2,07	TarBase, TargetScan Human, miRecords	RHEB	1
mmu-miR-155-5p	-2,07	miRecords	RHOA	1
mmu-miR-155-5p	-2,07	miRecords	RIPK1	1
mmu-miR-155-5p	-2,07	Ingenuity Expert Findings, TargetScan Human	SATB1	1
mmu-miR-155-5p	-2,07	TarBase	SCAMP1	1
mmu-miR-155-5p	-2,07	TarBase, TargetScan Human	SDCBP	1
mmu-miR-155-5p	-2,07	TarBase	SH3BP4	1
mmu-miR-155-5p	-2,07	Ingenuity Expert Findings, TargetScan Human	SLA	1
mmu-miR-155-5p	-2,07	TarBase	SLC30A1	1
mmu-miR-155-5p	-2,07	TarBase, TargetScan Human	SMAD1	1
mmu-miR-155-5p	-2,07	TargetScan Human, miRecords	SMAD2	1
mmu-miR-155-5p	-2,07	TarBase	SNAP29	1
mmu-miR-155-5p	-2,07	Ingenuity Expert Findings, TargetScan Human, miRecords	SOCS1	1
mmu-miR-155-5p	-2,07	Ingenuity Expert Findings, TarBase, TargetScan Human, miRecords	SPI1	1
mmu-miR-155-5p	-2,07	TarBase	SYNE2	1

mmu-miR-155-5p	-2,07	TarBase, TargetScan Human	SYPL1	1
mmu-miR-155-5p	-2,07	Ingenuity Expert Findings, TargetScan Human, miRecords	TAB2	1
mmu-miR-155-5p	-2,07	TarBase	TACSTD2	1
mmu-miR-155-5p	-2,07	TarBase	TBCA	1
mmu-miR-155-5p	-2,07	Ingenuity Expert Findings, TargetScan Human	TCF7L2	1
mmu-miR-155-5p	-2,07	TarBase, miRecords	TM6SF1	1
mmu-miR-155-5p	-2,07	TarBase	TNFRSF10A	1
mmu-miR-155-5p	-2,07	Ingenuity Expert Findings, TarBase, TargetScan Human, miRecords	TP53INP1	1
mmu-miR-155-5p	-2,07	TarBase, TargetScan Human	TRAM1	1
mmu-miR-155-5p	-2,07	TarBase, TargetScan Human	TRIM32	1
mmu-miR-155-5p	-2,07	TarBase, TargetScan Human	TRIP13	1
mmu-miR-155-5p	-2,07	TarBase	TXNDC12	1
mmu-miR-155-5p	-2,07	TarBase	TXNRD1	1
mmu-miR-155-5p	-2,07	TarBase	UBE2J1	1
mmu-miR-155-5p	-2,07	TarBase	UFL1	1
mmu-miR-155-5p	-2,07	TarBase	VAMP3	1
mmu-miR-155-5p	-2,07	TarBase	WDFY1	1
mmu-miR-155-5p	-2,07	Ingenuity Expert Findings, TargetScan Human	WEE1	1
mmu-miR-429-3p	-2,23	TargetScan Human, miRecords	BAP1	1
mmu-miR-429-3p	-2,23	miRecords	ELMO2	1
mmu-miR-429-3p	-2,23	miRecords	ERBB2IP	1
mmu-miR-429-3p	-2,23	TargetScan Human, miRecords	ERRFI1	1
mmu-miR-429-3p	-2,23	Ingenuity Expert Findings, Ingenuity ExpertAssist Findings, TargetScan Human	FHOD1	1
mmu-miR-429-3p	-2,23	TarBase	GEMIN2	1
mmu-miR-429-3p	-2,23	miRecords	KLHL20	1
mmu-miR-429-3p	-2,23	Ingenuity Expert Findings, TargetScan Human	MARCKS	1
mmu-miR-429-3p	-2,23	Ingenuity Expert Findings, TargetScan Human	PLCG1	1
mmu-miR-429-3p	-2,23	Ingenuity Expert Findings, TargetScan Human	PPM1F	1
mmu-miR-429-3p	-2,23	Ingenuity Expert Findings, TargetScan Human	PTEN	1
mmu-miR-429-3p	-2,23	Ingenuity Expert Findings, TargetScan Human	PTPN12	1
mmu-miR-429-3p	-2,23	Ingenuity Expert Findings, TargetScan Human	PTPN13	1
mmu-miR-429-3p	-2,23	miRecords	PTPRD	1
mmu-miR-429-3p	-2,23	miRecords	RERE	1
mmu-miR-429-3p	-2,23	TargetScan Human, miRecords	WASF3	1
mmu-miR-429-3p	-2,23	miRecords	WDR37	1
mmu-miR-429-3p	-2,23	TarBase, TargetScan Human, miRecords	ZEB1	1
mmu-miR-429-3p	-2,23	Ingenuity Expert Findings, TarBase, TargetScan Human, miRecords	ZEB2	1
mmu-miR-429-3p	-2,23	TargetScan Human, miRecords	ZFPM2	1
mmu-miR-212-5p	2,01	Ingenuity Expert Findings	PTCH1	-1
mmu-miR-214-3p	3,90	Ingenuity Expert Findings	ATF4	-1
mmu-miR-214-3p	3,90	Ingenuity Expert Findings, TargetScan Human	BAX	-1
mmu-miR-214-3p	3,90	miRecords	FGF16	-1
mmu-miR-214-3p	3,90	TargetScan Human, miRecords	GPD1	-1
mmu-miR-214-3p	3,90	Ingenuity Expert Findings, TargetScan Human	ING4	-1
mmu-miR-214-3p	3,90	TargetScan Human, miRecords	POU4F2	-1
mmu-miR-214-3p	3,90	Ingenuity Expert Findings, TarBase, miRecords	PTEN	-1

mmu-miR-214-3p	3,90	TargetScan Human, miRecords	SCN3A	-1
mmu-miR-30d-3p	-2,60	miRecords	AQP4	1
mmu-miR-30d-3p	-2,60	TarBase, miRecords	CDK6	1
mmu-miR-30d-3p	-2,60	TarBase, miRecords	CYR61	1
mmu-miR-30d-3p	-2,60	miRecords	FMR1	1
mmu-miR-30d-3p	-2,60	Ingenuity Expert Findings	HELZ	1
mmu-miR-30d-3p	-2,60	Ingenuity Expert Findings	PIK3C2A	1
mmu-miR-30d-3p	-2,60	TarBase, miRecords	SLC7A6	1
mmu-miR-30d-3p	-2,60	TarBase, miRecords	THBS1	1
mmu-miR-30d-3p	-2,60	TarBase, miRecords	TMEM2	1
mmu-miR-30d-3p	-2,60	TarBase, miRecords	TUBA1A	1
mmu-miR-30d-3p	-2,60	TarBase, miRecords	VEZT	1
mmu-miR-30d-3p	-2,60	Ingenuity Expert Findings	WDR44	1
mmu-miR-30d-3p	-2,60	TarBase, miRecords	WDR82	1
mmu-miR-30c-5p	-2,46	TargetScan Human, miRecords	ACVR1	1
mmu-miR-30c-5p	-2,46	TarBase	ADPGK	1
mmu-miR-30c-5p	-2,46	TarBase	ANPEP	1
mmu-miR-30c-5p	-2,46	TarBase, TargetScan Human	AP2A1	1
mmu-miR-30c-5p	-2,46	TarBase, TargetScan Human	ATP2A2	1
mmu-miR-30c-5p	-2,46	TarBase	ATRX	1
mmu-miR-30c-5p	-2,46	Ingenuity Expert Findings, TargetScan Human	BCL6	1
mmu-miR-30c-5p	-2,46	TargetScan Human, miRecords	BECN1	1
mmu-miR-30c-5p	-2,46	TarBase	C1orf56	1
mmu-miR-30c-5p	-2,46	TarBase, TargetScan Human	CBFB	1
mmu-miR-30c-5p	-2,46	TarBase	CDCP1	1
mmu-miR-30c-5p	-2,46	TarBase	CEP72	1
mmu-miR-30c-5p	-2,46	TarBase, TargetScan Human	CHD1	1
mmu-miR-30c-5p	-2,46	TarBase, TargetScan Human	CPNE8	1
mmu-miR-30c-5p	-2,46	Ingenuity Expert Findings	CTGF	1
mmu-miR-30c-5p	-2,46	TarBase, TargetScan Human	DOCK7	1
mmu-miR-30c-5p	-2,46	TarBase, TargetScan Human	ELMOD2	1
mmu-miR-30c-5p	-2,46	TarBase	F2	1
mmu-miR-30c-5p	-2,46	TarBase	FRG1	1
mmu-miR-30c-5p	-2,46	TarBase	FXR2	1
mmu-miR-30c-5p	-2,46	TarBase, TargetScan Human	GALNT1	1
mmu-miR-30c-5p	-2,46	TarBase, TargetScan Human	GALNT7	1
mmu-miR-30c-5p	-2,46	TarBase, TargetScan Human, miRecords	GNAI2	1
mmu-miR-30c-5p	-2,46	TarBase	GPD2	1
mmu-miR-30c-5p	-2,46	TarBase	HNRNPM	1
mmu-miR-30c-5p	-2,46	TarBase, TargetScan Human	IDH1	1
mmu-miR-30c-5p	-2,46	TarBase	IFRD1	1
mmu-miR-30c-5p	-2,46	TarBase	ITGA2	1
mmu-miR-30c-5p	-2,46	TarBase	JUN	1
mmu-miR-30c-5p	-2,46	TarBase	KDELC2	1
mmu-miR-30c-5p	-2,46	miRecords	KRT7	1
mmu-miR-30c-5p	-2,46	TarBase	KRT85	1
mmu-miR-30c-5p	-2,46	TarBase	LMNB2	1
mmu-miR-30c-5p	-2,46	TarBase, TargetScan Human	LRRC8C	1
mmu-miR-30c-5p	-2,46	TarBase	LTN1	1
mmu-miR-30c-5p	-2,46	Ingenuity Expert Findings, TargetScan Human	MAP4K4	1
mmu-miR-30c-5p	-2,46	TarBase, TargetScan Human	MAT2A	1

mmu-miR-30c-5p	-2,46	TarBase, TargetScan Human	MBNL1	1
mmu-miR-30c-5p	-2,46	TarBase	MET	1
mmu-miR-30c-5p	-2,46	TarBase	MLLT1	1
mmu-miR-30c-5p	-2,46	TarBase	MPDU1	1
mmu-miR-30c-5p	-2,46	TarBase	MYO10	1
mmu-miR-30c-5p	-2,46	TarBase, TargetScan Human	NAPG	1
mmu-miR-30c-5p	-2,46	TarBase, TargetScan Human	NCEH1	1
mmu-miR-30c-5p	-2,46	TarBase	NCL	1
mmu-miR-30c-5p	-2,46	TargetScan Human, miRecords	NEUROD1	1
mmu-miR-30c-5p	-2,46	TarBase	NPR3	1
mmu-miR-30c-5p	-2,46	TarBase	NT5C3A	1
mmu-miR-30c-5p	-2,46	TarBase, TargetScan Human	NT5E	1
mmu-miR-30c-5p	-2,46	TarBase	NUCB1	1
mmu-miR-30c-5p	-2,46	TarBase, TargetScan Human	NUFIP2	1
mmu-miR-30c-5p	-2,46	TarBase, TargetScan Human	P4HA2	1
mmu-miR-30c-5p	-2,46	TarBase, TargetScan Human	PAFAH1B2	1
mmu-miR-30c-5p	-2,46	TarBase	PEX11B	1
mmu-miR-30c-5p	-2,46	TarBase,TargetScan Human	PGM1	1
mmu-miR-30c-5p	-2,46	TarBase	PNP	1
mmu-miR-30c-5p	-2,46	TarBase	PPP2R4	1
mmu-miR-30c-5p	-2,46	TarBase, TargetScan Human	PPP3CA	1
mmu-miR-30c-5p	-2,46	TarBase, TargetScan Human	PRPF40A	1
mmu-miR-30c-5p	-2,46	TarBase, TargetScan Human	PTGFRN	1
mmu-miR-30c-5p	-2,46	TarBase, TargetScan Human	PTPRK	1
mmu-miR-30c-5p	-2,46	TarBase	PTRH1	1
mmu-miR-30c-5p	-2,46	TarBase, TargetScan Human	RAB27B	1
mmu-miR-30c-5p	-2,46	TarBase, TargetScan Human	RAD23B	1
mmu-miR-30c-5p	-2,46	TarBase	RBMS1	1
mmu-miR-30c-5p	-2,46	TarBase	RQCD1	1
mmu-miR-30c-5p	-2,46	Ingenuity Expert Findings, TargetScan Human	RUNX2	1
mmu-miR-30c-5p	-2,46	TarBase, TargetScan Human	SEC23A	1
mmu-miR-30c-5p	-2,46	TarBase, TargetScan Human	SEC62	1
mmu-miR-30c-5p	-2,46	TarBase	SLC12A4	1
mmu-miR-30c-5p	-2,46	TarBase, TargetScan Human	SLC38A1	1
mmu-miR-30c-5p	-2,46	TarBase, TargetScan Human	SLC38A2	1
mmu-miR-30c-5p	-2,46	TarBase	SLC4A10	1
mmu-miR-30c-5p	-2,46	TarBase, TargetScan Human	SLC4A7	1
mmu-miR-30c-5p	-2,46	TarBase	SLC7A1	1
mmu-miR-30c-5p	-2,46	TarBase, TargetScan Human	SLC7A11	1
mmu-miR-30c-5p	-2,46	TarBase	SLC9A3R2	1
mmu-miR-30c-5p	-2,46	TarBase	STRN	1
mmu-miR-30c-5p	-2,46	miRecords	STX1A	1
mmu-miR-30c-5p	-2,46	TarBase	STX7	1
mmu-miR-30c-5p	-2,46	TarBase, TargetScan Human	SYPL1	1
mmu-miR-30c-5p	-2,46	miRecords	SYT4	1
mmu-miR-30c-5p	-2,46	TarBase	THEM4	1
mmu-miR-30c-5p	-2,46	TarBase	TMCO1	1

mmu-miR-30c-5p	-2,46	TarBase	TMED10	1
mmu-miR-30c-5p	-2,46	TarBase	TMED2	1
mmu-miR-30c-5p	-2,46	TarBase	TMED3	1
mmu-miR-30c-5p	-2,46	TarBase	TMED7	1
mmu-miR-30c-5p	-2,46	TarBase	TMEM41B	1
mmu-miR-30c-5p	-2,46	TarBase	TMEM59	1
mmu-miR-30c-5p	-2,46	TarBase, TargetScan Human	TMEM87A	1
mmu-miR-30c-5p	-2,46	TarBase	TNFAIP2	1
mmu-miR-30c-5p	-2,46	TarBase, TargetScan Human	TNFRSF10B	1
mmu-miR-30c-5p	-2,46	TargetScan Human, miRecords	TNRC6A	1
mmu-miR-30c-5p	-2,46	miRecords	TP53	1
mmu-miR-30c-5p	-2,46	Ingenuity Expert Findings, TargetScan Human	TRPS1	1
mmu-miR-30c-5p	-2,46	TarBase	UAP1	1
mmu-miR-30c-5p	-2,46	TargetScan Human, miRecords	UBE2I	1
mmu-miR-30c-5p	-2,46	TarBase	WDR92	1
mmu-miR-30c-5p	-2,46	TarBase	WNT5A	1
mmu-miR-31-5p	-2,23	miRecords	CASR	1
mmu-miR-31-5p	-2,23	miRecords	CDKN2A	1
mmu-miR-31-5p	-2,23	TargetScan Human, miRecords	FOXP3	1
mmu-miR-31-5p	-2,23	miRecords	HIF1A	1
mmu-miR-31-5p	-2,23	TargetScan Human, miRecords	LATS2	1
mmu-miR-31-5p	-2,23	miRecords	PDGFB	1
mmu-miR-31-5p	-2,23	TargetScan Human, miRecords	PPP2R2A	1
mmu-miR-31-5p	-2,23	Ingenuity Expert Findings, TargetScan Human	SATB2	1
mmu-miR-31-5p	-2,23	Ingenuity Expert Findings, TargetScan Human	STK40	1
mmu-miR-9-5p	-2,36	TarBase, TargetScan Human, miRecords	BACE1	1
mmu-miR-9-5p	-2,36	Ingenuity Expert Findings, TargetScan Human, miRecords	CDH1	1
mmu-miR-9-5p	-2,36	miRecords	FGF16	1
mmu-miR-9-5p	-2,36	TargetScan Human,miRecords	FOXG1	1
mmu-miR-9-5p	-2,36	TargetScan Human,miRecords	FOXO1	1
mmu-miR-9-5p	-2,36	miRecords	NFKB1	1
mmu-miR-9-5p	-2,36	miRecords	NTRK3	1
mmu-miR-9-5p	-2,36	Ingenuity Expert Findings, TarBase, TargetScan Human, miRecords	ONECUT2	1
mmu-miR-9-5p	-2,36	miRecords	PMP22	1
mmu-miR-9-5p	-2,36	Ingenuity Expert Findings, TargetScan Human, miRecords	PRDM1	1
mmu-miR-9-5p	-2,36	TargetScan Human, miRecords	REST	1

Table-S3 List of regulated proteins identified by MS

Accession	Gene	ttest	LOG$_2$ Dicer$^{AQP2Cre+}$/Ctr
Q9WTK0	Nupr1	0,001082	-2,267222203
A0A5F8MQ17	Aqp4	0,01122	-2,016105512
Q3UM83	Klrg2	8,58E-07	-1,961535395
A0A0R4J0Z3	Aqp4	0,003202	-1,802907875
Q04573	Npy1r	2,7E-07	-1,562348061
P56402	Aqp2	0,000143	-1,507514338
Q8K078	Slco4a1	0,002214	-1,312348746
O35874	Slc1a4	0,000134	-1,237053873
Q91VV4	Dennd2d	0,000234	-1,236848404
F6VG99	Lmo7	0,000404	-1,183706822
Q61699	Hsph1	2,3E-06	-1,125186687
E9QMU3	Map7	0,000361	-1,117867881
Q8C0Z1	Fam234a	7,61E-06	-1,058626746
P22935	Crabp2	0,001503	-1,048319239
P48025	Syk	2,05E-05	-1,033456557
A2AJN7	Slc4a11	1,91E-06	-1,0234378
Q68FG2	Sptbn2	5,87E-07	-1,009099473
E9PYF4	Lmo7	9,25E-07	-0,997187939
Q8R4T9	Slc14a2	8,54E-05	-0,944310497
Q0VBK2	Krt80	2,1E-08	-0,915969053
Q99PS0	Krt23	3,34E-05	-0,873465892
Q9DAW9	Cnn3	4,09E-05	-0,848266217
D3YYS6	Mgll	1,05E-06	-0,822167058
E9Q557	Dsp	2,35E-06	-0,810926442
P46414	Cdkn1b	7,91E-06	-0,80299213
P34914	Ephx2	1,68E-05	-0,801973311
B1AWN4	Atp10b	2,43E-05	-0,789137833
P23927	Cryab	0,000157	-0,745589758
Q61696	Hspa1a	7,02E-05	-0,739658985
P59113	Fermt1	2,55E-06	-0,73204329
E9QN01	Nt5dc1	0,001042	-0,7283543
Q9JKZ2	Slc5a3	0,000474	-0,722825179
E9Q565	Myzap	0,000191	-0,721597193
Q9D6P8	Calml3	0,005835	-0,720751482
Q9D379	Ephx1	1,42E-05	-0,708486133
Q8VEE1	Lmcd1	7,15E-06	-0,705803336
Q7TPS5	C2cd5	0,000872	-0,702974929
Q80UW2	Fbxo2	0,000213	-0,699536714
P06801	Me1	3,16E-05	-0,686939085
P48722	Hspa4l	1,91E-05	-0,678306394

Accession	Gene	ttest	LOG_2 $Dicer^{AQP2Cre+}$/Ctr
Q80WC7	Agfg2	0,000834	-0,675727965
Q8K0T0	Rtn1	0,000224	-0,673291195
Q64669	Nqo1	4,99E-05	-0,667673552
Q9R0H2	Emcn	0,009058	-0,66659493
Q3UUY6	Prom2	0,001945	-0,660513534
Q8K157	Galm	0,000144	-0,655045206
A0A0G2JGD2	S100a4	4,8E-05	-0,651402225
D3Z2V6	Mras	0,000265	-0,644728718
Q3TLQ0	Map2	0,000261	-0,643752688
Q64314	Cd34	5,27E-05	-0,638298943
Q8K3K7	Agpat2	0,000101	-0,63213765
Q9Z0S5	Cldn15	0,000356	-0,626562457
Q3TGF2	Fam107b	5,11E-05	-0,625353125
P97770	Thumpd3	0,000287	-0,622568711
Q9JHW9	Aldh1a3	0,000127	-0,620279829
Q9EQ06	Hsd17b11	0,000236	-0,616655468
Q8BJY1	Psmd5	9,59E-06	-0,614240293
Q9DAV9	Tmem38b	0,001169	-0,613271624
G5E8R3	Pcx	0,000221	-0,612906708
Q4VAC9	Plekhg3	3,25E-05	-0,611222516
Q9JJV2	Pfn2	6,87E-05	-0,609286956
O88844	Idh1	1,59E-05	-0,606635843
A1L3P4	Slc9a6	8E-05	-0,606032905
Q9DCE5	Pak1ip1	0,005916	-0,605430019
E9Q4X5	Eps8l1	3,65E-05	-0,604827185
D3Z3N4	Hnrnph3	1,23E-06	-0,60338244
Q3UJU9	Rmdn3	1,39E-06	-0,60338244
B2RSU6	Cgnl1	2,16E-06	-0,601937704
Q99KB8	Hagh	1,65E-05	-0,601813794
F8WGT1	Ahcyl2	0,00113	-0,600732448
P12246	Apcs	0,00329	0,601211271
D3Z3L3	Trim12c	0,000988	0,604827185
P19324	Serpinh1	0,000677	0,607602921
Q8BSH3	Tpm1	0,006154	0,607841877
A0A2I3BQZ9	App	0,000714	0,609286956
P26645	Marcks	0,003482	0,609651319
Q61391	Mme	6,84E-06	0,619547868
Q70UZ7	Vwa2	0,000424	0,620884076
F6UIS1	Ergic3	0,007134	0,623539533
Q9EPB4	Pycard	0,001997	0,625353125
P06909	Cfh	0,00247	0,628009623
Q2YDW2	Msto1	0,003789	0,630321867
P30275	Ckmt1	0,001102	0,633585751
Q8R0Y6	Aldh1l1	0,000967	0,634191192
Q9JHP7	Poglut2	0,003214	0,636007846

Accession	Gene	ttest	LOG$_2$ Dicer$^{AQP2Cre+}$/Ctr
Q8R3G9	Tspan8	0,000324	0,6467845
Q61739	Itga6	0,00083	0,649952135
B1AU74	Mospd2	9,63E-06	0,651773145
P97298	Serpinf1	0,001027	0,651773145
Q8BMK4	Ckap4	0,000187	0,6544379
Q9Z1E4	Gys1	0,003199	0,659905712
F6ZQA3	Numa1	0,000554	0,660141273
O89086	Rbm3	0,000609	0,661121413
Q3V0K9	Pls1	0,000753	0,664396968
F7D4H5	Phactr2	0,002002	0,676337305
G5E874	Lamc2	0,001547	0,682433975
P16294	F9	4,33E-05	0,686705204
Q07797	Lgals3bp	0,001177	0,686939085
Q9Z0E6	Gbp2	0,000318	0,689147232
Q9DBK7	Uba7	0,000348	0,692201131
G3X8S6	Bicc1	5E-05	0,704199205
E9Q3E2	Synpo	0,000218	0,704199205
Q9Z0J1	Reck	0,011036	0,705742357
O08691	Arg2	0,000912	0,713621499
Q60675	Lama2	0,001499	0,71484783
P08074	Cbr2	0,004008	0,71630649
P98078	Dab2	0,002673	0,716687802
Q07113	Igf2r	1,96E-05	0,717069216
E9Q7G0	Numa1	1,03E-06	0,717682767
A0A1L1SSH9	Sparc	0,003439	0,724899193
Q8C6E0	Cfap36	0,00096	0,729583704
Q9JK53	Prelp	6,58E-05	0,730198503
E9PX59	Samd9l	6,76E-05	0,744973315
Q9JKY7	Cyp2d22	8,71E-05	0,749519889
Q9EQH2	Erap1	4,25E-06	0,758550534
O35206	Col15a1	0,001817	0,772160671
G3UZ26	Shmt1	0,010688	0,789531421
Q64449	Mrc2	3,97E-05	0,791789886
Q05186	Rcn1	0,003048	0,804918846
P35330	Icam2	0,009281	0,805711535
O35074	Ptgis	5,91E-06	0,810076133
P52800	Efnb2	0,004732	0,818816201
Q8BMF3	Me3	0,003373	0,830074999
Q9CSH3	Dis3	0,000483	0,834685212
Q80X19	Col14a1	0,004177	0,835086798
Q9WTQ5	Akap12	0,00144	0,851409233
E9QB01	Ncam1	0,001008	0,857477271
Q8BKG3	Ptk7	0,000113	0,85770117
Q60766	Irgm1	0,000233	0,880195729
Q6NVD0	Frem2	0,002191	0,89371899

Accession	Gene	ttest	LOG_2 $Dicer^{AQP2Cre+}$/Ctr
Q9QXS6	Dbn1	3,28E-05	0,9083287
Q8VCC9	Spon1	0,000101	0,911510676
Q920Q8	Ivns1abp	4,64E-05	0,932566049
P28667	Marcksl1	0,000122	0,933205581
O35309	Nmi	0,000105	0,937885861
Q922K9	Frk	0,000138	0,941966306
Q99PG2	Ogfr	1,41E-06	0,961652257
Q91YN9	Bag2	1,33E-05	0,966585323
A2APT9	Klhdc7a	0,003538	0,969163255
Q8CAS9	Parp9	1,08E-07	0,969807971
Q9R233	Tapbp	6,84E-05	0,999134556
P23249	Mov10	0,000427	1,005413496
H3BLI9	Tsc22d1	0,000425	1,0069298
Q91VF6	Col26a1	0,000407	1,00736402
P01901	H2-K1	0,000316	1,009966096
P01899	H2-D1	0,00015	1,026049971
P17918	Pcna	0,000707	1,042412873
Q99K94	Stat1	7,64E-06	1,055993834
F6VRP8	Lgals3bp	0,000346	1,0828245
Q9WTK5	Nfkb2	0,000127	1,103618134
Q61233	Lcp1	0,000401	1,144434018
G3X9T7	Lgals9	0,002678	1,153397676
Q5DU00	Dcdc2	0,000199	1,153862836
D3YTX1	Npnt	9,05E-07	1,175711115
P49717	Mcm4	0,003554	1,194334191
Q9QZ85	Iigp1	0,001839	1,195223251
P28076	Psmb9	0,000651	1,197269294
Q3TBA3	Tap1	0,000342	1,214430432
O89053	Coro1a	0,000974	1,243752801
O08746	Matn2	8E-05	1,261767468
P36371	Tap2	0,000313	1,309530527
A0A171EBL2	Rnf213	2,62E-05	1,331231922
D3Z5N2	Stmn1	0,003766	1,34401628
Q91X17	Umod	0,000326	1,347576232
P35441	Thbs1	0,000132	1,354194509
Q640N1	Aebp1	0,000342	1,36328578
P82198	Tgfbi	0,001092	1,385029624
P28063	Psmb8	0,000463	1,425435943
Q61635	Ifi47	4,68E-05	1,456973456
F6R2G3	Muc4	0,000811	1,473233644
Q64339	Isg15	0,000231	1,491462069
Q64282	Ifit1	0,000101	1,607554854
Q61881	Mcm7	0,000187	1,616875416
Q8CFZ6	Clec3b	0,000904	1,658223356
P24549	Aldh1a1	1,19E-05	1,665528623

Accession	Gene	ttest	LOG_2 $Dicer^{AQP2Cre+}$/Ctr
Q9DCE9	Igtp	0,000461	1,666130624
A0A087WQM1	Serpine2	0,001947	2,275515361
A0A0R4J086	Olfml3	0,001535	2,551175326

Table-S4 List of the significantly regulated miRNA/protein target pair

ID	FDR	Log_2 Ratio	Source	ID	Symbol	Log_2 Ratio	Regulation
mmu-miR-141-3p	0,000853	-1,15	TargetScan Human	Q91YN9	BAG2	0,967	miRNA Down – Protein Up
mmu-miR-141-3p	0,000853	-1,15	TargetScan Human	Q61739	ITGA6	0,65	miRNA Down – Protein Up
mmu-miR-141-5p	0,0315	-0,782	TargetScan Human	P98078	DAB2	0,717	miRNA Down – Protein Up
mmu-miR-141-5p	0,0315	-0,782	TargetScan Human	P52800	EFNB2	0,819	miRNA Down – Protein Up
mmu-miR-148a-3p	0,0000368	-0,961	TargetScan Human	G3X8S6	BICC1	0,704	miRNA Down – Protein Up
mmu-miR-148a-3p	0,0000368	-0,961	TargetScan Human	Q5DU00	DCDC2	1,154	miRNA Down – Protein Up
mmu-miR-148a-3p	0,0000368	-0,961	TargetScan Human	P52800	EFNB2	0,819	miRNA Down – Protein Up
mmu-miR-148a-3p	0,0000368	-0,961	TargetScan Human	P01899	HLA-A	1,026	miRNA Down – Protein Up
mmu-miR-148a-3p	0,0000368	-0,961	TargetScan Human	O35309	NMI	0,938	miRNA Down – Protein Up
mmu-miR-148a-3p	0,0000368	-0,961	TargetScan Human	F7D4H5	PHACTR2	0,676	miRNA Down – Protein Up
mmu-miR-155-5p	0,026	-1,048	TarBase	B1AU74	MOSPD2	0,652	miRNA Down – Protein Up
mmu-miR-155-5p	0,026	-1,048	TargetScan Human	F7D4H5	PHACTR2	0,676	miRNA Down – Protein Up
mmu-miR-15a-5p	0,0141	-0,813	TargetScan Human	Q9WTQ5	AKAP12	0,851	miRNA Down – Protein Up
mmu-miR-15a-5p	0,0141	-0,813	TargetScan Human	A0A2I3BQZ9	APP	0,609	miRNA Down – Protein Up
mmu-miR-15a-5p	0,0141	-0,813	TargetScan Human	P52800	EFNB2	0,819	miRNA Down – Protein Up
mmu-miR-15a-5p	0,0141	-0,813	TarBase	Q07113	IGF2R	0,717	miRNA Down – Protein Up
mmu-miR-15a-5p	0,0141	-0,813	TargetScan Human	Q61233	LCP1	1,144	miRNA Down – Protein Up
mmu-miR-15a-5p	0,0141	-0,813	TargetScan Human	P23249	MOV10	1,005	miRNA Down – Protein Up
mmu-miR-15a-5p	0,0141	-0,813	TargetScan Human	F7D4H5	PHACTR2	0,676	miRNA Down – Protein Up
mmu-miR-15a-5p	0,0141	-0,813	TargetScan Human	Q3V0K9	PLS1	0,664	miRNA Down – Protein Up
mmu-miR-15a-5p	0,0141	-0,813	TargetScanHuman, miRecords	Q9Z0J1	RECK	0,706	miRNA Down – Protein Up
mmu-miR-15a-5p	0,0141	-0,813	TarBase	A0A087WQM1	SERPINE2	2,276	miRNA Down – Protein Up
mmu-miR-15a-5p	0,0141	-0,813	TargetScan Human	Q91X17	UMOD	1,348	miRNA Down – Protein Up
mmu-miR-15a-5p	0,0141	-0,813	TargetScan Human	A0A0R4J0R1	VAMP8	0,953	miRNA Down – Protein Up
mmu-miR-187-3p	0,0000186	-1,191	TargetScan Human	P98078	DAB2	0,717	miRNA Down – Protein Up
mmu-miR-187-3p	0,0000186	-1,191	TargetScan Human	P52800	EFNB2	0,819	miRNA Down – Protein Up
mmu-miR-187-3p	0,0000186	-1,191	TargetScan Human	P97298	SERPINF1	0,652	miRNA Down – Protein Up
mmu-miR-194-5p	0,00288	-1,173	TargetScan Human	P52800	EFNB2	0,819	miRNA Down – Protein Up
mmu-miR-194-5p	0,00288	-1,173	TargetScan Human	A0A087WQM1	SERPINE2	2,276	miRNA Down – Protein Up
mmu-miR-194-5p	0,00288	-1,173	TargetScan Human	P35441	THBS1	1,354	miRNA Down – Protein Up
mmu-miR-429-3p	0,00000678	-1,155	TargetScan Human	Q8BMK4	CKAP4	0,654	miRNA Down – Protein Up
mmu-miR-429-3p	0,00000678	-1,155	TargetScan Human	F7D4H5	PHACTR2	0,676	miRNA Down – Protein Up

ID	FDR	Log_2 Ratio	Source	ID	Symbol	Log_2 Ratio	Regulation
mmu-miR-429-3p	0,00000678	-1,155	TargetScan Human	Q9JHP7	POGLUT2	0,636	miRNA Down − Protein Up
mmu-miR-429-3p	0,00000678	-1,155	TargetScan Human	Q9Z0J1	RECK	0,706	miRNA Down − Protein Up
mmu-miR-429-3p	0,00000678	-1,155	TargetScan Human	H3BLI9	TSC22D1	1,007	miRNA Down − Protein Up
mmu-miR-224-5p	0,0217	-0,845	TargetScan Human	P01899	HLA-A	1,026	miRNA Down − Protein Up
mmu-miR-26a-5p	0,00492	-0,652	TargetScan Human	A0A2I3BQZ9	APP	0,609	miRNA Down − Protein Up
mmu-miR-26a-5p	0,00492	-0,652	TargetScan Human	Q5DU00	DCDC2	1,154	miRNA Down − Protein Up
mmu-miR-26a-5p	0,00492	-0,652	TargetScan Human	Q9CSH3	DIS3	0,835	miRNA Down − Protein Up
mmu-miR-26a-5p	0,00492	-0,652	TargetScan Human	Q05186	RCN1	0,805	miRNA Down − Protein Up
mmu-miR-26a-5p	0,00492	-0,652	TargetScan Human	D3Z5N2	STMN1	1,344	miRNA Down − Protein Up
mmu-miR-26a-5p	0,00492	-0,652	TargetScan Human	Q3TBA3	TAP1	1,214	miRNA Down − Protein Up
mmu-miR-29a-3p	0,0000762	-0,952	TarBase, TargetScan Human, miRecords	O35206	COL15A1	0,772	miRNA Down − Protein Up
mmu-miR-29a-3p	0,0000762	-0,952	TargetScan Human	Q80T14	FRAS1	0,756	miRNA Down − Protein Up
mmu-miR-29a-3p	0,0000762	-0,952	TargetScan Human	Q6NVD0	FREM2	0,894	miRNA Down − Protein Up
mmu-miR-29a-3p	0,0000762	-0,952	TargetScan Human	Q61739	ITGA6	0,65	miRNA Down − Protein Up
mmu-miR-29a-3p	0,0000762	-0,952	TargetScan Human	Q60675	LAMA2	0,715	miRNA Down − Protein Up
mmu-miR-29a-3p	0,0000762	-0,952	TargetScan Human	O35309	NMI	0,938	miRNA Down − Protein Up
mmu-miR-29a-3p	0,0000762	-0,952	TargetScan Human	F7D4H5	PHACTR2	0,676	miRNA Down − Protein Up
mmu-miR-29a-3p	0,0000762	-0,952	TargetScan Human	Q9JHP7	POGLUT2	0,636	miRNA Down − Protein Up
mmu-miR-29a-3p	0,0000762	-0,952	TargetScan Human	P19324	SERPINH1	0,608	miRNA Down − Protein Up
mmu-miR-29a-3p	0,0000762	-0,952	Ingenuity Expert Findings, TarBase, TargetScan Human, miRecords	A0A1L1SSH9	SPARC	0,725	miRNA Down − Protein Up
mmu-miR-29a-3p	0,0000762	-0,952	Ingenuity Expert Findings, miRecords	Q8BSH3	Tpm1	0,608	miRNA Down − Protein Up
mmu-miR-30d-3p	0,0000238	-1,378	TargetScan Human	B1AU74	MOSPD2	0,652	miRNA Down − Protein Up
mmu-miR-30d-3p	0,0000238	-1,378	TargetScan Human	F7D4H5	PHACTR2	0,676	miRNA Down − Protein Up
mmu-miR-30d-3p	0,0000238	-1,378	TargetScan Human	A2AQ51	SLC12A1	0,836	miRNA Down − Protein Up
mmu-miR-30d-3p	0,0000238	-1,378	TarBase,miRecords	P35441	THBS1	1,354	miRNA Down − Protein Up
mmu-miR-30b-3p	0,00103	-1,16	TargetScan Human	O35206	COL15A1	0,772	miRNA Down − Protein Up
mmu-miR-30b-3p	0,00103	-1,16	TargetScan Human	F7D4H5	PHACTR2	0,676	miRNA Down − Protein Up
mmu-miR-30b-3p	0,00103	-1,16	TargetScan Human	Q3V0K9	PLS1	0,664	miRNA Down − Protein Up
mmu-miR-30b-3p	0,00103	-1,16	TargetScan Human	D3Z5N2	STMN1	1,344	miRNA Down − Protein Up

ID	FDR	Log_2 Ratio	Source	ID	Symbol	Log_2 Ratio	Regulation
mmu-miR-30c-1-3p	0,00138	-0,97	TargetScan Human	P98078	DAB2	0,717	miRNA Down – Protein Up
mmu-miR-30c-1-3p	0,00138	-0,97	TargetScan Human	P28667	MARCKSL1	0,933	miRNA Down – Protein Up
mmu-miR-30c-1-3p	0,00138	-0,97	TargetScan Human	Q61881	MCM7	1,617	miRNA Down – Protein Up
mmu-miR-30c-1-3p	0,00138	-0,97	TargetScan Human	P19324	SERPINH1	0,608	miRNA Down – Protein Up
mmu-miR-30c-1-3p	0,00138	-0,97	TargetScan Human	Q99K94	STAT1	1,056	miRNA Down – Protein Up
mmu-miR-30c-1-3p	0,00138	-0,97	TargetScan Human	Q9R233	TAPBP	0,999	miRNA Down – Protein Up
mmu-miR-30c-1-3p	0,00138	-0,97	TargetScan Human	D3Z3L3	TRIM5	0,605	miRNA Down – Protein Up
mmu-miR-30c-5p	4,83E-09	-1,301	TargetScan Human	Q61739	ITGA6	0,65	miRNA Down – Protein Up
mmu-miR-30c-5p	4,83E-09	-1,301	TargetScan Human	Q61233	LCP1	1,144	miRNA Down – Protein Up
mmu-miR-30c-5p	4,83E-09	-1,301	TargetScan Human	P23249	MOV10	1,005	miRNA Down – Protein Up
mmu-miR-30c-5p	4,83E-09	-1,301	TargetScan Human	F7D4H5	PHACTR2	0,676	miRNA Down – Protein Up
mmu-miR-30c-5p	4,83E-09	-1,301	Ingenuity Expert Findings	A0A1L1SSH9	SPARC	0,725	miRNA Down – Protein Up
mmu-miR-30c-5p	4,83E-09	-1,301	Ingenuity Expert Findings	Q8BSH3	Tpm1	0,608	miRNA Down – Protein Up
mmu-miR-31-5p	0,0000338	-1,157	TargetScan Human	A0A2I3BQZ9	APP	0,609	miRNA Down – Protein Up
mmu-miR-31-5p	0,0000338	-1,157	TargetScan Human	Q9JK53	PRELP	0,73	miRNA Down – Protein Up
mmu-miR-31-5p	0,0000338	-1,157	TargetScan Human	A0A1L1SSH9	SPARC	0,725	miRNA Down – Protein Up
mmu-miR-31-5p	0,0000338	-1,157	TargetScan Human	P36371	TAP2	1,31	miRNA Down – Protein Up
mmu-miR-455-3p	0,0000238	-1,674	TargetScan Human	P24549	ALDH1A1	1,666	miRNA Down – Protein Up
mmu-miR-455-3p	0,0000238	-1,674	TargetScan Human	Q8CAS9	PARP9	0,97	miRNA Down – Protein Up
mmu-miR-455-3p	0,0000238	-1,674	TargetScan Human	Q05186	RCN1	0,805	miRNA Down – Protein Up
mmu-miR-455-3p	0,0000238	-1,674	TargetScan Human	A0A0R4J0R1	VAMP8	0,953	miRNA Down – Protein Up
mmu-miR-664-5p	0,0115	-0,991	TargetScan Human	Q91VF6	COL26A1	1,007	miRNA Down – Protein Up
mmu-miR-664-5p	0,0115	-0,991	TargetScan Human	O89053	CORO1A	1,244	miRNA Down – Protein Up
mmu-miR-664-5p	0,0115	-0,991	TargetScan Human	P28667	MARCKSL1	0,933	miRNA Down – Protein Up
mmu-miR-664-5p	0,0115	-0,991	TargetScan Human	P23249	MOV10	1,005	miRNA Down – Protein Up
mmu-miR-664-5p	0,0115	-0,991	TargetScan Human	F7D4H5	PHACTR2	0,676	miRNA Down – Protein Up
mmu-miR-664-5p	0,0115	-0,991	TargetScan Human	Q9JK53	PRELP	0,73	miRNA Down – Protein Up
mmu-miR-664-5p	0,0115	-0,991	TargetScan Human	O35074	PTGIS	0,81	miRNA Down – Protein Up
mmu-miR-664-5p	0,0115	-0,991	TargetScan Human	O89086	RBM3	0,661	miRNA Down – Protein Up
mmu-miR-664-5p	0,0115	-0,991	TargetScan Human	Q9D939	SULT1C2	0,967	miRNA Down – Protein Up
mmu-miR-664-5p	0,0115	-0,991	TargetScan Human	Q91X17	UMOD	1,348	miRNA Down – Protein Up
mmu-miR-1943-5p	0,0141	-1,022	TargetScan Human	O08691	ARG2	0,714	miRNA Down – Protein Up
mmu-miR-1943-5p	0,0141	-1,022	TargetScan Human	Q9QXS6	DBN1	0,908	miRNA Down – Protein Up
mmu-miR-1943-5p	0,0141	-1,022	TargetScan Human	P52800	EFNB2	0,819	miRNA Down – Protein Up

ID	FDR	Log_2 Ratio	Source	ID	Symbol	Log_2 Ratio	Regulation
mmu-miR-1943-5p	0,0141	-1,022	TargetScan Human	D3YTX1	NPNT	1,176	miRNA Down − Protein Up
mmu-miR-1943-5p	0,0141	-1,022	TargetScan Human	A0A0R4J086	OLFML3	2,551	miRNA Down − Protein Up
mmu-miR-1943-5p	0,0141	-1,022	TargetScan Human	Q9JK53	PRELP	0,73	miRNA Down − Protein Up
mmu-miR-1943-5p	0,0141	-1,022	TargetScan Human	Q3TBA3	TAP1	1,214	miRNA Down − Protein Up
mmu-miR-1943-5p	0,0141	-1,022	TargetScan Human	Q9R233	TAPBP	0,999	miRNA Down − Protein Up
mmu-miR-9-5p	0,00000166	-1,237	TargetScan Human	O08691	ARG2	0,714	miRNA Down − Protein Up
mmu-miR-9-5p	0,00000166	-1,237	TargetScan Human	O35206	COL15A1	0,772	miRNA Down − Protein Up
mmu-miR-9-5p	0,00000166	-1,237	TargetScan Human	Q6NVD0	FREM2	0,894	miRNA Down − Protein Up
mmu-miR-9-5p	0,00000166	-1,237	TargetScan Human	F7D4H5	PHACTR2	0,676	miRNA Down − Protein Up
mmu-miR-9-5p	0,00000166	-1,237	TargetScan Human	D3Z5N2	STMN1	1,344	miRNA Down − Protein Up
mmu-miR-9-5p	0,00000166	-1,237	TargetScan Human	P82198	TGFBI	1,385	miRNA Down − Protein Up
mmu-miR-1247-5p	6,14E-08	2,611	TargetScan Human	Q80WC7	AGFG2	-0,676	miRNA Up − Protein Down
mmu-miR-1247-5p	6,14E-08	2,611	TargetScan Human	Q61646	HP	-0,902	miRNA Up − Protein Down
mmu-miR-1247-5p	6,14E-08	2,611	TargetScan Human	Q9WTK0	NUPR1	-2,267	miRNA Up − Protein Down
mmu-miR-212-3p	0,000407	1,361	TargetScan Human	Q9R0H2	EMCN	-0,667	miRNA Up − Protein Down
mmu-miR-212-3p	0,000407	1,361	TargetScan Human	Q61696	HSPA1A/HSPA1B	-0,74	miRNA Up − Protein Down
mmu-miR-143-5p	0,0485	1,026	TargetScan Human	D3Z2V6	MRAS	-0,645	miRNA Up − Protein Down
mmu-miR-145a-5p	0,00191	0,987	TargetScan Human	A0A5F8MQ17	AQP4	-2,016	miRNA Up − Protein Down
mmu-miR-145a-5p	0,00191	0,987	TargetScan Human	P97770	THUMPD3	-0,623	miRNA Up − Protein Down
mmu-miR-181c-3p	0,0239	0,739	TargetScan Human	Q64314	CD34	-0,638	miRNA Up − Protein Down
mmu-miR-184-3p	0,0341	0,632	TargetScan Human	Q8BXK9	CLIC5	-0,654	miRNA Up − Protein Down
mmu-miR-184-3p	0,0341	0,632	TargetScan Human	P22935	CRABP2	-1,048	miRNA Up − Protein Down
mmu-miR-184-3p	0,0341	0,632	TargetScan Human	Q9D379	EPHX1	-0,708	miRNA Up − Protein Down
mmu-miR-184-3p	0,0341	0,632	TargetScan Human	Q8R4T9	SLC14A2	-0,944	miRNA Up − Protein Down
mmu-miR-193b-3p	0,0174	0,937	TargetScan Human	P56402	AQP2	-1,508	miRNA Up − Protein Down
mmu-miR-193b-3p	0,0174	0,937	TargetScan Human	Q64314	CD34	-0,638	miRNA Up − Protein Down
mmu-miR-193b-3p	0,0174	0,937	TargetScan Human	B2RSU6	CGNL1	-0,602	miRNA Up − Protein Down
mmu-miR-193b-3p	0,0174	0,937	TargetScan Human	A0A338P6K2	MYH11	-0,672	miRNA Up − Protein Down
mmu-miR-193b-3p	0,0174	0,937	TargetScan Human	O35874	SLC1A4	-1,237	miRNA Up − Protein Down
mmu-miR-193b-3p	0,0174	0,937	TargetScan Human	Q9JKZ2	SLC5A3	-0,723	miRNA Up − Protein Down
mmu-miR-212-5p	0,0344	1,008	TargetScan Human	Q8BXK9	CLIC5	-0,654	miRNA Up − Protein Down
mmu-miR-212-5p	0,0344	1,008	TargetScan Human	Q80UW2	FBXO2	-0,7	miRNA Up − Protein Down
mmu-miR-212-5p	0,0344	1,008	TargetScan Human	Q61699	HSPH1	-1,125	miRNA Up − Protein Down
mmu-miR-212-5p	0,0344	1,008	TargetScan Human	Q68FG2	SPTBN2	-1,009	miRNA Up − Protein Down
mmu-miR-214-3p	0,00000158	1,965	TargetScan Human	B2RSU6	CGNL1	-0,602	miRNA Up − Protein Down

ID	FDR	Log_2 Ratio	Source	ID	Symbol	Log_2 Ratio	Regulation
mmu-miR-214-3p	0,00000158	1,965	TargetScan Human	Q8C0Z1	FAM234A	-1,059	miRNA Up – Protein Down
mmu-miR-214-3p	0,00000158	1,965	TargetScan Human	E9Q0F0	KRT78	-1,066	miRNA Up – Protein Down
mmu-miR-214-3p	0,00000158	1,965	TargetScan Human	O35874	SLC1A4	-1,237	miRNA Up – Protein Down
mmu-miR-214-3p	0,00000158	1,965	TargetScan Human	Q68FG2	SPTBN2	-1,009	miRNA Up – Protein Down
mmu-miR-34c-5p	0,00889	0,708	TargetScan Human	Q9D6P8	CALML3	-0,721	miRNA Up – Protein Down
mmu-miR-34c-5p	0,00889	0,708	TargetScan Human	P46414	CDKN1B	-0,803	miRNA Up – Protein Down
mmu-miR-34c-5p	0,00889	0,708	TargetScan Human	Q9Z0S5	CLDN15	-0,627	miRNA Up – Protein Down
mmu-miR-34c-5p	0,00889	0,708	TargetScan Human	Q8BXK9	CLIC5	-0,654	miRNA Up – Protein Down
mmu-miR-34c-5p	0,00889	0,708	TargetScan Human	P22935	CRABP2	-1,048	miRNA Up – Protein Down
mmu-miR-34c-5p	0,00889	0,708	TargetScan Human	Q8C0Z1	FAM234A	-1,059	miRNA Up – Protein Down
mmu-miR-34c-5p	0,00889	0,708	TargetScan Human	Q8K157	GALM	-0,655	miRNA Up – Protein Down
mmu-miR-34c-5p	0,00889	0,708	TargetScan Human	P51661	HSD11B2	-1,079	miRNA Up – Protein Down
mmu-miR-34c-5p	0,00889	0,708	TargetScan Human	Q61696	HSPA1A/HSPA1B	-0,74	miRNA Up – Protein Down
mmu-miR-34c-5p	0,00889	0,708	TargetScan Human	O88844	IDH1	-0,607	miRNA Up – Protein Down
mmu-miR-34c-5p	0,00889	0,708	TargetScan Human	D3Z2V6	MRAS	-0,645	miRNA Up – Protein Down
mmu-miR-34c-5p	0,00889	0,708	TargetScan Human	Q8BJY1	PSMD5	-0,614	miRNA Up – Protein Down
mmu-miR-34c-5p	0,00889	0,708	TargetScan Human	Q9JKZ2	SLC5A3	-0,723	miRNA Up – Protein Down
mmu-miR-540-3p	0,044	0,873	TargetScan Human	Q9JHW9	ALDH1A3	-0,62	miRNA Up – Protein Down
mmu-miR-540-3p	0,044	0,873	TargetScan Human	Q64314	CD34	-0,638	miRNA Up – Protein Down
mmu-miR-540-3p	0,044	0,873	TargetScan Human	Q9Z0S5	CLDN15	-0,627	miRNA Up – Protein Down

Materials and Methods

Animal experiment

Targeted inactivation of Dicer1 in the CD.

Ablation of the Dicer1 gene in the CD was performed by mating AQP2Cre/+ mice, expressing CRE under the control of the endogenous AQP2 promoter,1 with Dicer1flox/+ mice in which exons 22-23 of the Dicer1 gene were flanked by loxP sites.2 Dicer1flox/flox; AQP2Cre/+ mice, termed DicerAQP2Cre+, were used as the experimental group, while littermate mice with no CRE expression, DicerAQP2Cre- mice, served as controls. All animal experiments were performed in a temperature and humidity controlled environment, with a 12 h day/night light cycle. Male and female mice were used. Genotyping and confirmation of Dicer excision were performed by PCR analysis using genomic DNA isolated from ear snips and renal tissue. All primers are listed in Table S1.

Physiological studies

All the procedures involving animals were conducted as indicated in the Italian National Guidelines (D.L. N° 116 G.U., suppl. 40, 18.2.1992, circ. N° 8, G.U. July 1994) and in the appropriate European Directives (EEC Council Directive 86/609, 1.12.1987) under an approved animal license (ID n°547/2017-PR). Mouse renal function was investigated by housing the mice individually in metabolic cages. After a period of adjustment, water intake was examined and 24-hour urine samples were collected under mineral oil. Urinary volume, osmolality, together with serum and urine electrolytes were evaluated.

dDAVP administration test. To investigate their urinary concentrating ability, mice were challenged with the vasopressin analog 1-deamino, 8-D arginine-vasopressin (dDAVP Sigma Aldrich, St. Louis, MO, USA) as described previously.3 Briefly, after voiding the bladder on a cold plate an i.p. injection of vehicle (NaCl 0.9%) or dDAVP (1 µg/kg of body weight (BW) dissolved in equal volume of vehicle was administered. Urine volume and osmolality were evaluated after 5 hours of urine collection in metabolic cages.

Amiloride administration test. Mice were housed individually in metabolic cages for 5 days and fed a NaCl-restricted diet (UPAE, INRA, France). To assess ENaC-dependent sodium reabsorption, mice were challenged with the selective inhibitor of ENaC, amiloride.4 Vehicle or 1.45 mg/kg BW amiloride hydrochloride (Sigma Aldrich, St. Louis, MO, USA) was injected i.p for two consecutive days and urine collected after 6 hours.

cAMP detection in urine and inner medulla. Tissue and urinary cAMP content was measured using an ELISA (Cayman Chemical, Ann Arbor, MI, #581001). The IM was homogenized in 5 % trichloroacetic acid,5 in water and then centrifuged at 1,500 x g for 10 minutes for debrids removal. TCA was removed using water-satured ether and heating the samples at 70°C for five minutes. Total protein concentration was measured by a BCA assay and cAMP level was expressed as pmol/mg of protein. Urine samples were centrifuged for 5 min at 2,300 x g, diluted in enzyme immunoassay buffer and assayed directly following the manufacturers' instructions. cAMP content was expressed in nmol/mg of urinary creatinine.

Small RNA sequencing and data processing

Total RNA was extracted from IM (3 control and 3 DicerAQP2Cre+ mice) with the RNeasy Micro Kit (Qiagen, Milan, Italy, #74004) according to the manufacturer's protocol. The RNA concentration was assessed by Nanodrop, Qubit and a Bioanalyzer. The library was generated from 1 µg of RNA using a TruSeq small-RNA protocol (Illumina Way, San Diego, CA, USA, #200-0036), which was sequenced to obtain 50 base pair single-reads on the Illumina HiSeq2500 Platform, with 20 million reads / sample. Data quality was checked using

FASTQC v0.11.3 (https://github.com/golharam/FastQC). Data were processed using the iMir tool (https://tools4mirs.org/software/isomirs_identification/imir/) to remove the adapter sequence and reads with at least 15 nucleotides were retained and mapped to the mouse genome (build mm9) to identify miRNAs according to miRBase v.21 (http://www.mirbase.org/) annotations as previously shown,6 (Fig.S1). Data normalization and differential expression analysis were performed using DESeq2 R package, removing features with less than 3 read counts per sample. The raw data of the small RNA sequencing have been added to GEO database (accession GSE161006) and are accessible at: https://www.ncbi.nlm.nih.gov/geo/query/acc.cgi?acc=GSE161006.

Proteomic analysis

Dissected mouse IM tissue from both control and the DicerAQP2Cre+ mice were processed for LC-MS/MS analysis. Tandem Mass Tag (TMT) labeling, randomly assigned between the two sample sets, (as described,7) was used to facilitate protein quantification. Mass spectrometry was carried out on a Tribrid Fusion mass spectrometer (Thermo Scientific) using the MS3 collection to allow accurate protein quantification.8 Data were searched using SEQUEST against the uniprot mouse protein database (dated 25-03-2020) and quantified using Proteome discoverer 2.4. Protein quantification was based only on unique peptides. Proteins were considered significantly regulated when they passed the Benjamini-Hochberg FDR of 0.05. The mass spectrometry proteomics data have been deposited to the ProteomeXchange Consortium via the PRIDE,9 partner repository with the dataset identifier PXD022327.

Bioinformatics

Differentially expressed miRNAs (DicerAQP2Cre+ vs control, FDR corrected Wald test p-value ≤ 0.05 and expression absolute fold change ≥ 2) were assessed by Ingenuity Pathway Analysis software (Qiagen Bioinformatics, Redwood City, CA, USA) to identify potential regulators, relationships, mechanisms, functions, and pathways relevant to the observed changes (an adjusted $P \leq 0.05$). TargetScan Mouse 7.1 and mirBase v.21 were used for target prediction and miRNAs sequence identification, respectively. The identification of transcription factor (TFs) binding sites was performed by in silico computational analysis of the 1000bp 5'-flanking region of the AQP2 gene using the MatInspector software tool (Genomatix database, https://www.genomix4life.com/it/) 10. The miRNA/protein expression scatter graph was generated in R by plotting for each miRNA/target pair the expression fold change of miRNA (y-axis) and corresponding target protein identified by the proteomic analysis (x-axis). All miRNas with log2 ratio > or < 0.6 were used as imputs. The predicted targets proteins of these miRNAs (Targetscan, Injenuity Expert Findings, miRrecords, TarBase) were compared with the entire proteome. Common identified found in the predicted and "real" list) were plotted according their expression fold change. The dots falling in the top/left and in the bottom/right sections of the graph represented the miRNA-Up/Protein-Down (green) and the miRNA-Down/Protein-Up pairs (red), respectively. The cut-off threshold used for up and down regulated miRNAs and proteins was log2 > or < 0.6 FDR 0.05.

miRNA mimics transfection in mpkCCD14 cells

Three miRNAs (miR-7688-5p, miR-8114 and miR-409-3p) were selected for in vitro validation of the software based prediction based on their predicted targets being involved both in transcription factor and epigenetic regulation (Fig.S2). mpkCCD14 cells (subclone

11),10 were routinely cultured as described.11 Cells were seeded at a density of 2 x 105 cells/cm2 on semi-permeable filters (Transwell, 0.4 µm pore size, Corning, #3450). When 80% confluent they were transfected with 10 nM miRNA mimics (mirVana miRNA mimics; mmu-miR-7688-5p, mmu-miR-8114, mmu-miR-409-3p) and Lipofectamine 2000 (Invitrogen, Carlsbad, CA, USA, #11668019) according to manufacturer's guidelines. Transfection efficiency was evaluated by testing different concentrations of lipofectamine and a Cy5-conjugated miRNA-409,12 (Fig-S3). Cells were cultured for an additional 7 days, before incubation in serum-free media for 24 h, then an additional 24 h with dDAVP (1nM).13 Total RNA was isolated using Ambion Ribopure kit (Invitrogen, Carlsbad, CA, USA, #10107824).

Constructs and luciferase assay

The 3'-UTR regions of AQP2, GATA2 and GATA3 were amplified by PCR from mouse genomic DNA, using the following primers: AQP2 fw AATTTCTAGAGTCGGTTCCCAGTGCAGG; AQP2 rev AATTTCTAGAGAAACACGCAGA-GATGGACG; GATA2 fw ATTTCTAGACCCGCATAAGAGAAGAATCG; GATA2 rev AATT-TCTAGAGGGTAGCATACAATTTTTACAGACAA; GATA3 fw AATTTCTAGACAGGGTCT-CTAGTGCTGTGAAA; GATA3 rev AATTTCTAGAGGCCTAGCCATGACATTCTC. PCR products were cloned downstream of the luc+ gene in the pGL3-Control vector (Promega Corporation, Milan, Italy, #E1741) using XbaI. All plasmids were sequenced for confirmation. HEK293 cells in 24 well plates were transiently transfected with the plasmids with siPORT (Ambion Life Technologies, Paisley, UK, # AM4510) in the presence of mature microRNA-7688-5p, microRNA-8114, and microRNA-409-3p mimics (final concentration of 100 nM) and assessed after 48 h. To generate the AQP2 promoter construct, a 840bp fragment containing the mouse AQP2 promoter was amplified by PCR using the primers: AQP2 promoter fw GTACTAGGTACCTCATGTACACAGGCAGAGCA; AQP2 promoter rev GTACTAGCTAGCCGGAGAGGCTAGACTGTGG. This fragment was cloned into the pGL3-basic vector (Promega Corporation, Milan, Italy, #E1751) between KpnI and NheI restriction sites, upstream of the luc+ gene. The promoter containing plasmid was transiently transfected into HEK293 cells alongside microRNA-8114 and microRNA-409-3p mimics (as above). Luciferase activity was assayed with a dual luciferase assay system (Promega Corporation, Milan, Italy, #E1500) as described in the manufacturer's instructions. Briefly, the activities of Firefly and Renilla luciferases were measured in sequence from each sample and expressed as ratio Firefly/Renilla. In case of miRNA binding to the 3' UTR of the putative target gene, a reduction of Firefly luciferase activity (due to the instability of the fused mRNA) compared to the control sample (non-targeting scrambled oligonucleotide transfection) is detected. In this way, the firefly luciferase activity serve as positive control of the miRNA to mRNA interaction. Luminescence was measured for 10s using a 2103 EnVision Multilabel Plate Reader (Perkin Elmer).

Quantitative ChIP analysis

For the protein-DNA binding analysis, mouse IMs were cross-linked as previously described.14 ChIP assays were performed using the ChromaFlash High-Sensitivity ChIP Kit (Epigentek Group Inc., Farmingdale, NY, USA). Antibodies used for Protein-DNA immunoprecipitation were: anti-GRC5/PHF2 (Abcam Inc. #Ab124434), anti-KDM5C5c (Abcam Inc. #Ab194288). Non-Immune IgG and anti-RNA Polymerase II were used as negative and positive control antibodies, respectively. DNA was subjected to RT-qPCR using iQTM SYBR® Green PCR Supermix (BIO RAD). Amplification of the Aqp2 promoter fragment was performed using the primers: forward AQP2ChF (position from nucleotides -

71 to -88) 5'-CACAGGGTTGGCAGGAAC-3' and reverse AQP2ChR (position from nucleotides -29 to -49): 5'- GGCCTTCCTATCGTAGACCTG-3'. The primers away from Aqp2 TSS were used for RT-qPCR negative control of binding: forward AQP2NCF (position from nucleotides-2725 to -2753): 5'- AAAGCAAACACGGGAGGAT-3' and reverse AQP2NCR (position from nucleotides -2562 to -2587) 5'- CTTCATGCCAGGGAAGCA-3'. (Fig-6A). All RT-qPCR signals from immunoprecipitated DNA were normalized to RT-qPCR signals from non-immunoprecipitated input DNA. Results are expressed as percentage of the input, and graphs represent mean values ± SD of 3 independent experiments. Asterisks (*) indicate statistically significant differences with p-value obtained through a 2way ANOVA (*p<0.05; **p<0.01; **p<0.001; DicerAQPCre+ mice and controls, and IgG vs. antibody).

Immunohistochemistry

All the procedures for immunohistochemistry were according to our previous study.15 Briefly, after anesthesia with isofluorane, arterial blood was collected via the abdominal aorta and the left kidney was collected. The right kidney was fixed by anterograde perfusion through the abdominal aorta with 4% paraformaldehyde (PFA). The kidney was isolated and after progressive dehydration in ethanol solutions (70%, 96%, 99%) it was incubated overnight in xylene, before embedding in paraffin. For histological analysis, 4 μm thick sections were stained with Hematoxylin and Eosin (Sigma-Aldrich, St. Louis, MO, USA). For immunofluorescence, after rehydration of sections, target retrieval was performed in TEG buffer pH 9.2,15 and sections were incubated with primary antibodies overnight at 4°C. The following primary antibodies were used; goat anti-AQP2 (Santa Cruz Biotechnology, Dallas, TX, USA, #sc-9882) 1:300; rabbit anti-B1H+-ATPase (Santa Cruz Biotechnology, Dallas, TX, USA, #sc-20943,) 1:500; rabbit anti-AQP4 (alomone labs, Jerusalem, Israel #249-323) 1:500; rabbit anti-αENaC (StressMarq, Victoria, BC, Canada, #SPC-403) 1:1000; anti-p256 AQP2 1:750.16 The following secondary antibodies were incubated for 1 h at room temperature; rabbit anti-Goat IgG (H+L) AlexaFluo 488 (A-11078 Thermo Fisher Scientific, Waltham, MA, USA); 1:400; goat anti-rabbit IgG Cy3 (Thermo Fisher Scientific, Waltham, MA, USA, #A10520) 1:800. Sections were mounted with fluorescent mounting medium (Dako, Carpinteria, CA, USA). Images were acquired with a Zeiss spinning disk Axio Observer Z1 confocal microscope (Zeiss, Oberkochen, Germany).

Immunoblotting

Immunoblotting from tissue samples was performed as described.17 Briefly, kidneys were dissected into cortex/outer-stripe of outer medulla (OSOM), inner-stripe of outer medulla (ISOM) and inner medulla (IM). Kidneys were homogenized with a Tissue Lyser RETSCH MM300 (Qiagen, Milan, Italy) in lysis buffer (sucrose 0.3 M, imidazole 25 mM, EDTA 1 mM, PMSF 1 mM) with protease (Santa Cruz, Dallas, TX, USA, Complate Protease Inhibitor Cocktail,) and phosphatase inhibitor cocktails (Roche, Monza, Italy, PhosSTOP). Total protein concentration was measured by a BCA assay. SDS-PAGE was performed on NuPage 4-12% Bis-Tris Gel (Waltham, MA, USA) or on home-made gels (stacking gel: 0.5M Tris-HCl pH 6.8, acrylamide/bis 30%, 10% sodium dodecyl sulfate (SDS) 0.1%, ammonium peroxodisulfate (APS) 0.1%, tetramethylethylenediamine (TEMED) 0.1%, resolving gel: 1.5M Tris-HCl pH8.8, 10% SDS0.1%, APS 0.1%, TEMED 0.1%). Proteins were transferred to PVDF or nitrocellulose membranes (Invitrogen, Waltham, MA, USA). Membranes were incubated overnight with primary antibodies at 4°C, washed, and subsequently incubated with secondary antibody for 1 hour at room temperature. Proteins were visualized using enhanced chemiluminescence (Thermo Fisher Scientific, Waltham, MA, USA, Pierce, ECL Western Blotting, #32106). Densitometry was performed using ImageJ software.

Immunoblotting for mpkCCD14 cells differed only in the lysis buffer (20 mM Tris, 150 mM NaCl, 1% Nonidet P-40, 5 mM EDTA (pH 7.4), 20 mM N-ethylmaleimide (Sigma), 22 μM PR619 (Abcam), 5 μg/ml leupeptin, 100 μg/ml Pefabloc, and PhosSTOP phosphatase inhibitor tablets (Roche Diagnostics), in which the cells were sonicated soon after the treatment as described below. The following primary antibodies were used: rabbit anti-AQP2 (7661AP)Y,18 kindly provided by Prof. Sebastian Frische); mouse anti-B1/2 H+ATPase (Biotechnology, Dallas, TX, USA, #sc-55544) 1:1000; rabbit anti-α-ENaC (StressMarq, Victoria, BC, Canada, #SPC-403) 1:5000; anti-β-Actin (Sigma, Milan, Italy, #A2066) 1:20000; anti-p256AQP2 (K0307AP) 1:500, p261AQP2,19 1:500, anti-Km5c (ab194288, abcam) 1:1000 and anti-Phf2 (ab124434, abcam) 1:1000. The following secondary antibodies were used at 1:2000 dilution: anti-mouse HRP conjugated (GE Healthcare, Little Chalfont, UK, # NA931V) and goat anti-rabbit 1:5000 (GE Healthcare, Little Chalfont, UK, #NA934V).

Cortical Collecting Duct isolation

Tubule isolation was performed as previously detailed.20 Briefly, kidneys from one-month old mice were perfused through the abdominal aorta with 1ml of perfusion solution containing 1mg/ml collagenase type IV Collagenase type IV (Worthington – USA origin) (PAN Biotech, Aidenbach, Germany, # LS0004186) and 1mg/ml protease type XIV (Sigma Aldrich, Milan, Italy, #P5147). The whole harvested kidney was minced into 1 mm3 slices and incubated at 37°C under shaking (850rpm) in 1ml of digestion solution containing 1 mg/ml collagenase type II (Worthington – USA origin) (PAN Biotech, Aidenbach, Germany, # collagenase type II) and 1 mg/ml protease type XIV (Sigma Aldrich, Milan, Italy, #P5147). After 10 min, a 500 µl aliquot of digested tubules was transferred into 500 µl of ice-cold tubule isolation buffer containing 0.5 mg/ml albumin. Digestion of the remaining tubule suspension was continued by adding an additional 500 µl of isolation buffer and the sample was incubated at 37°C under shaking for an additional 5 min before collection of a new aliquot. These steps were repeated until 5 different aliquots were collected. Collecting ducts were then manually isolated from the different aliquots with aid of a stereo microscope.

Real time quantitative PCR (RT-qPCR)

Total RNA was isolated from tissues and isolated tubules using TRIsure reagent (BIOLINE, A Meridian life Science® Company, WilfongRdMemphis, TN, USA, # BIO-38033). 1µg of RNA was reverse-transcribed by Quantitect Reverse Transcription Kit (Qiagen, Milan, Italy, # 205311) according to the manufacturer's instructions. The RT-qPCR was performed with the FG Power SYBR Green PCR Master Mix (Applied Biosystems, Waltham, MA, USA) according to the manufacturer's instructions. Fold changes were calculated by the ΔΔCt method,21 using GAPDH levels for normalization. Primer sequences are listed in Table S1. Validation of inner medulla miRNAs was performed using the miRVana miRNA Isolation Kit (Ambion, Austin, TX, USA, #AM1560). 100 ng of RNA was reverse-transcribed by TaqMan MicroRNA Reverse Transcription Kit (Applied Biosystems, Waltham, MA, USA, #4366597) and a miRNA-specific primer according to the manufacturer's instructions. TaqMan MicroRNA Assays (Applied Biosystems, Waltham, MA, USA, #4427975) were performed according to the manufacturer's instructions and specific TaqMan Micro Assays primers were used. All quantifications were normalized with the sno135 RNA level and the fold induction was calculated by the ΔΔCt method.21 For miRNA detection in mpkCCD cells (see below), a universal stem loop primer containing a tail with 8 random nucleotides was used,22 (Table 2). For each reaction the annealing temperature was 62°C. All quantifications (ΔCt) were normalized with 18S tRNA levels and the fold induction was calculated by the ΔΔCt method. Primer sequences are listed in Table S1.

Multiphoton microscopy label-free fibrosis evaluation

Unstained paraffin-embedded 4 μm thick sections were used. Two photon images were recorded using an upright Ultima Investigator 2-photon microscope (Bruker, MS, USA) equipped with Ti-Sapphire laser (Mai Tai® DeepSee™, Spectra-Physics, USA) and a 20X objective (XLUMPlanFL20XW) NA 1.0, (Olympus, Japan). The fibrillar collagen was detectable from second harmonic generation signal.23 SHG and 2 photon excitation fluorescence (2PEF) were simultaneously excited by tuning the laser to 900 nm. Emitted light between 500 and 550 nm (green channel) and between 435 and 485 nm (blue channel) was recorded using Hamamatsu model H10770PB-40 GaAsP-detector and Hamamatsu model R3896 multi-alkali detector, respectively.

Statistical analysis

Values are shown as mean ± SEM or SD as stated in the figure legend. Comparison between two groups was made by unpaired t-test or one or two way ANOVA as indicated in the figure legend. A p-value < 0.05 was considered significant.

Reference List

1. Ronzaud C, Loffing J, Bleich M, et al. Impairment of sodium balance in mice deficient in renal principal cell mineralocorticoid receptor. J Am Soc Nephrol. 2007;18(6): 1679-1687.
2. Murchison EP, Partridge JF, Tam OH, Cheloufi S, Hannon GJ. Characterization of Dicer-deficient murine embryonic stem cells. Proc. Natl. Acad. Sci. U. S. A. 2005;102(34): 12135-12140.
3. Trepiccione F, Gerber SD, Grahammer F, et al. Renal Atp6ap2/(Pro)renin Receptor Is Required for Normal Vacuolar H+-ATPase Function but Not for the Renin-Angiotensin System. J Am Soc Nephrol. 2016;27(11): 3320-3330.
4. Sinning A, Radionov N, Trepiccione F, et al. Double Knockout of the Na+-Driven Cl-/HCO3- Exchanger and Na+/Cl- Cotransporter Induces Hypokalemia and Volume Depletion. J Am Soc Nephrol. 2017;28(1): 130-139.
5. Veitenhansl M, Stegner K, Hierl FX, et al. 40th EASD Annual Meeting of the European Association for the Study of Diabetes : Munich, Germany, 5-9 September 2004. Diabetologia. 2004;47(Suppl 1): A1-A464.
6. Pellegrini KL, Gerlach CV, Craciun FL, et al. Application of small RNA sequencing to identify microRNAs in acute kidney injury and fibrosis. Toxicol Appl Pharmacol. 2016;312: 42-52.
7. Wu A, Wolley MJ, Wu Q, Gordon RD, Fenton RA, Stowasser M. The Cl(-)/HCO3(-) exchanger pendrin is downregulated during oral co-administration of exogenous mineralocorticoid and KCl in patients with primary aldosteronism. J Hum Hypertens. 2020.
8. Ting L, Rad R, Gygi SP, Haas W. MS3 eliminates ratio distortion in isobaric multiplexed quantitative proteomics. Nat Methods. 2011;8(11): 937-940.
9. Perez-Riverol Y, Csordas A, Bai J, et al. The PRIDE database and related tools and resources in 2019: improving support for quantification data. Nucleic Acids Res. 2019;47(D1): D442-D450.
10. Yu MJ, Miller RL, Uawithya P, et al. Systems-level analysis of cell-specific AQP2 gene expression in renal collecting duct. Proc. Natl. Acad. Sci. U. S. A. 2009;106(7): 2441-2446.
11. Moeller HB, Slengerik-Hansen J, Aroankins T, et al. Regulation of the Water Channel Aquaporin-2 via 14-3-3theta and -zeta. J Biol Chem. 2016;291(5): 2469-2484.
12. Alabdullah AA, Al-Abdulaziz B, Alsalem H, et al. Estimating transfection efficiency in differentiated and undifferentiated neural cells. BMC Res Notes. 2019;12(1): 225.
13. Kim JE, Jung HJ, Lee YJ, Kwon TH. Vasopressin-regulated miRNAs and AQP2-targeting miRNAs in kidney collecting duct cells. Am J Physiol Renal Physiol. 2015;308(7): F749-764.
14. Angrisano T, Pero R, Brancaccio M, et al. Cyclical DNA Methylation and Histone Changes Are Induced by LPS to Activate COX-2 in Human Intestinal Epithelial Cells. PLoS One. 2016;11(6): e0156671.
15. Trepiccione F, Altobelli C, Capasso G, Christensen BM, Frische S. Lithium increases ammonium excretion leading to altered urinary acid-base buffer composition. J Nephrol. 2018;31(3): 385-393.
16. Moeller HB, Aroankins TS, Slengerik-Hansen J, Pisitkun T, Fenton RA. Phosphorylation and ubiquitylation are opposing processes that regulate endocytosis of the water channel aquaporin-2. J Cell Sci. 2014;127(Pt 14): 3174-3183.
17. Iervolino A, De La Motte LR, Petrillo F, et al. Integrin Beta 1 Is Crucial for Urinary Concentrating Ability and Renal Medulla Architecture in Adult Mice. Front Physiol. 2018;9: 1273.
18. Nielsen J, Kwon TH, Praetorius J, Frokiaer J, Knepper MA, Nielsen S. Aldosterone increases urine production and decreases apical AQP2 expression in rats with diabetes insipidus. Am J Physiol Renal Physiol. 2006;290(2): F438-449.

19. Hoffert JD, Fenton RA, Moeller HB, et al. Vasopressin-stimulated increase in phosphorylation at Ser269 potentiates plasma membrane retention of aquaporin-2. J Biol Chem. 2008;283(36): 24617-24627.
20. Hofmeister MV, Fenton RA, Praetorius J. Fluorescence isolation of mouse late distal convoluted tubules and connecting tubules: effects of vasopressin and vitamin D3 on Ca2+ signaling. Am J Physiol Renal Physiol. 2009;296(1): F194-203.
21. Livak KJ, Schmittgen TD. Analysis of relative gene expression data using real-time quantitative PCR and the 2(-Delta Delta C(T)) Method. Methods. 2001;25(4): 402-408.
22. Yang LH, Wang SL, Tang LL, et al. Universal stem-loop primer method for screening and quantification of microRNA. PLoS One. 2014;9(12): e115293.
23. Aref-Eshghi E, Schenkel LC, Lin H, et al. The defining DNA methylation signature of Kabuki syndrome enables functional assessment of genetic variants of unknown clinical significance. Epigenetics. 2017;12(11): 923-933.